

## Journal Pre-proofs

Facile synthesis of 1,2,3-triazole-fused Indolo- and Pyrrolo[1,4]diazepines, DNA-binding and evaluation of their anticancer activity

Jitendra Gour, Srikanth Gatadi, Venkatesh Pooladanda, Shaik Mohammad Ghose, Satyaveni Malasala, Y.V. Madhavi, Chandraiah Godugu, Srinivas Nanduri

PII: S0045-2068(19)31025-9  
DOI: <https://doi.org/10.1016/j.bioorg.2019.103306>  
Reference: YBIOO 103306

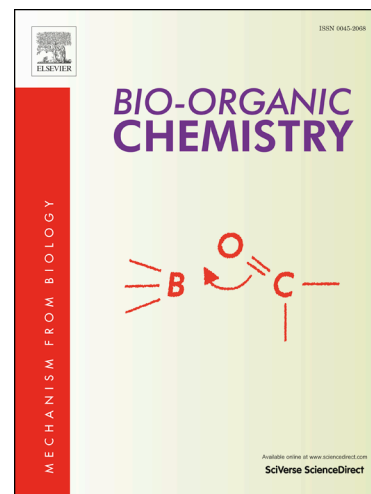
To appear in: *Bioorganic Chemistry*

Received Date: 27 June 2019  
Revised Date: 17 September 2019  
Accepted Date: 19 September 2019

Please cite this article as: J. Gour, S. Gatadi, V. Pooladanda, S. Mahammad Ghose, S. Malasala, Y.V. Madhavi, C. Godugu, S. Nanduri, Facile synthesis of 1,2,3-triazole-fused Indolo- and Pyrrolo[1,4]diazepines, DNA-binding and evaluation of their anticancer activity, *Bioorganic Chemistry* (2019), doi: <https://doi.org/10.1016/j.bioorg.2019.103306>

This is a PDF file of an article that has undergone enhancements after acceptance, such as the addition of a cover page and metadata, and formatting for readability, but it is not yet the definitive version of record. This version will undergo additional copyediting, typesetting and review before it is published in its final form, but we are providing this version to give early visibility of the article. Please note that, during the production process, errors may be discovered which could affect the content, and all legal disclaimers that apply to the journal pertain.

© 2019 Published by Elsevier Inc.



# Facile synthesis of 1,2,3-triazole-fused Indolo- and Pyrrolo[1,4]diazepines, DNA-binding and evaluation of their anticancer activity

Jitendra Gour,<sup>a</sup> Srikanth Gatadi,<sup>a</sup> Venkatesh Pooladanda,<sup>b</sup> Shaik Mahammad Ghouse,<sup>a</sup> Satyaveni Malasala,<sup>a</sup> Y.V. Madhavi,<sup>a</sup> Chandraiah Godugu,<sup>b</sup> and Srinivas Nanduri\*<sup>a</sup>

<sup>a</sup>*Department of Medicinal Chemistry, National Institute of Pharmaceutical Education and Research (NIPER) Hyderabad 500 037, India*

<sup>b</sup>*Department of Pharmacology and Toxicology, National Institute of Pharmaceutical Education and Research (NIPER), Hyderabad 500 037, India*

**Abstract:** A facile synthetic strategy has been developed for the generation of structurally diverse *N*-fused heterocycles. The formation of fused 1,2,3-triazole indolo and pyrrolodiazepines proceeds through an initial Knoevenagel condensation followed by intramolecular azide–alkyne cycloaddition reaction at room temperature without recourse to the traditional Cu(I)-catalyzed azide–alkyne cycloadditions. The synthesized compounds were evaluated for their *in vitro* anti-cancer activity against the NCI 60 cell line panel. Among the tested compounds, **3a** and **3h** were found to exhibit potent inhibitory activity against many of the cell lines. Cell cycle analysis indicated that the compounds inhibit the cell cycle at sub G1 phase. The DNA- nano drop method, viscosity experiment and docking studies suggested these compounds possess DNA binding affinity.

**Keywords:** Fused polycyclics; Cytotoxicity; DNA-binding; MDA-MB-468 cancer cells

**\*Corresponding author.\***Dr.Srinivas Nanduri, Tel: +91-40-23073740; Fax: +91-40-23073751; E-mail: [nandurisrini92@gmail.com](mailto:nandurisrini92@gmail.com)

Journal Pre-proofs

## Introduction

Cancer is a major public health concern, responsible for an estimated 9.6 million deaths in 2018 globally [1]. The World Health Organization (WHO) reported that about 1 in 6 deaths globally are due to cancer. Therefore, development of new heterocyclic compounds with potent anti-cancer properties continues to be the major area of research [2]. Chemotherapeutic agents targeting DNA, such as groove binders, DNA alkylating agents, or intercalators are found to be the most effective when used in combination with drugs that have different mechanisms of action [3]. DNA-intercalators consisting of polycyclic planar moieties could insert between adjacent base pairs of a DNA molecule without disturbing the overall stacking pattern [4]. However, the selectivity could be improved by introduction of specific substituents on the intercalative aromatic core.

Indole and pyrrole fused polycyclics [5] represent some of the most versatile and privileged scaffolds [6] occupying important position in medicinal and synthetic organic chemistry owing to their unique structural features and promising pharmacological properties [7]. Particularly, indole and pyrrole fused seven-member diazepine class of compounds are known to possess interesting biological properties [8]. For example, the diazepino-indole derivatives are reported to exhibit melanin concentrating hormone receptor 1 activity [9]. Lixivaptan [10], a pyrrolo-diazepine is in clinical development for cardiovascular diseases (Phase III). Structurally related polycyclic fused indoles are known to possess antitumor, estrogen receptor modulation, tubulin polymerization inhibitory and kinase inhibitory activities [11]. On the other hand, 1,2,3-triazoles particularly condensed with heterocycles are known to exhibit a broad range of biological activities including anticancer, anti-HIV, anti-inflammatory and antibacterial activities [12]. Benzo[*e*]pyrrolo[1,2-*a*][1,2,3]triazolo[5,1-*c*][1,4]diazepin-8(4*H*)-one is known to exhibit protease

inhibitory activity, (+)-JQ-1 [13] and I-BET762 [14] are potent inhibitors of bromodomain and extra-C terminal domain (BET) proteins. Benzo-pyrido-triazolo-diazepines [15] are used as effective anti-cancer compounds. Pyrrolo[2,1-*c*][1,4]benzodiazepines (PBDs) exert their cytotoxic and antitumor activity through covalent binding to DNA [16,17] (**figure 1**). To broaden the scope of this class of compounds, we designed a series of new 1,2,3-triazole-fused indolo- and pyrrolo[1,4]diazepines, where the triazole ring is fused to diazepine moiety. The presence of a larger aromatic system can lead to a higher affinity for the DNA molecule and consequently to a greater growth inhibitory potency. Additionally, 1,2,3-triazole frameworks possess striking connections in biological systems because of their remarkable metabolic stability and ability to form hydrogen bonding to biomolecular targets [18]. Doxorubicin and Dactinomycin drugs are under clinical use for the treatment of different types of cancers which act through DNA intercalation [18c].

<Insert **Figure 1** here>

A perusal of literature indicated limited number of reports on synthesis and biological profile of indole and pyrrole fused diazepines [19]. In 2008, Fujii and Ohno described the synthesis of indole 1,2-fused benzo-1,4-diazepines via copper-catalyzed domino three component cyclization from *N*-mesyl-2-ethynylanilines [20]. Hajela et al. reported a tandem C-2 functionalization followed by intramolecular azide-alkyne 1,3-dipolar cycloaddition reaction to access pyrrolotriazolodiazepines [19b]. In 2015, Balci and co-workers pioneered the use of gold-catalyzed and NaH-supported intramolecular cyclization of *N*-propargyl indoles with pyrazole and pyrrole attached to indole at C2 position to generate pyrazolodiazepinoindole, pyrazolopyrazinoindole and pyrrolopyrazinoindole (**scheme 1a**) [21]. Kurth et al. developed an Indium (III)-

catalyzed one-pot MCR for the synthesis of imidazotriazolobenzodiazepines (**Scheme 1b**) [22]. Sun and co-workers demonstrated a palladium-catalyzed synthesis of 1,2-fused-indole diazepines via [5+2] annulation of *O*-indolo anilines with alkynes [19a].

<Insert **Scheme 1** here>

Among the various approaches, copper and Ru-catalyzed intramolecular azide-alkyne cascade reactions have proven to be versatile method for the construction of diverse 1,2,3-triazole fused *N*-heterocycles. However, copper(I) and Ru possess undesirable side effects even in low concentrations [23]. Thus, there exists a need for developing metal free and easily accessible methods. But the metal free reaction conditions normally require high temperatures (>100 °C) or use some other methods like microwave or photo catalysis [24]. Hence, a convenient and novel strategy for an efficient construction of these frameworks is greatly desirable. As part of our continued interest toward the design and synthesis of fused polycyclic indole and pyrrole derivatives [25], we aimed at direct synthesis of polycyclic heteroaromatic compounds **3** via reaction of 1-(prop-2-yn-1-yl)-1*H*-indole-2-carbaldehyde with different substituted phenacylazides under basic conditions in a one pot operation (**Scheme 1c**). To the best of our knowledge, 1,2,3-Triazole-fused indolo and pyrrolo(1,4 diazepine) have not been reported so far. We report herein the details of the synthesis, biological studies, DNA binding properties, and molecular modelling of the new compounds.

## Results and Discussion

### Chemistry

*N*-propargyl indole and pyrrole derivatives are useful precursors for intramolecular cyclizations. The initial reaction was conducted with 1-(prop-2-yn-1-yl)-1*H*-indole-2-

carbaldehyde **1a** (0.5 mmol) and 2-azido-1-phenylethan-1-one **2a** (0.6 mmol) in presence of Cs<sub>2</sub>CO<sub>3</sub> (1.0 mmol) in ethanol at room temperature for 24 hours. The desired product (4*H*-[1,2,3]triazolo[5',1':3,4][1,4]diazepino[1,7-*a*]indol-12-yl)(phenyl)methanone **3a** was obtained in low, but isolable, 15% yield (Table 1, entry 1). When the same reaction was repeated using KO<sup>*t*</sup>Bu as base, the anticipated, 1,2,3-triazole-fused indolo-[1,4]diazepine product **3a** did not form even after 48 hours (Table 1, entry 2). For further improvement, we turned our attention to investigate different inorganic and organic bases. No significant improvement in the formation of the product was observed when K<sub>2</sub>CO<sub>3</sub>, KOH and NaOH were used (Table 1, entries 3–6). **3a** was obtained in 62% yield when the reaction was carried out in ethanol as solvent and TEA as a base (Table 1, entry 7). When the solvent was changed to methanol, the product was obtained in comparable yields (65%; Table 1, entry 8). However, when DMF was used as solvent **3a** was obtained in low yield (38%; Table 1, entry 9). When the base was changed to DBU and methanol as solvent, the yield further decreased. (Table 1, entry 10). When piperidine was used as base (1.0 mmol), the reaction completed in 28 hours and **3a** was obtained in nearly quantitative yield 79% (Table 1, entry 11). Increase of the reaction time did not improve the yield (Table 1, entry 12). When the concentration of piperidine is reduced to 0.5 mmol, the yield was found to be the best 81% (Table 1, entry 13). Further reduction in the concentration of piperidine (0.4 mmol) resulted in loss of yield (Table 1, entry 14). When the reaction was conducted at higher temperatures (70 °C) the yield was found to be less (42%, entry 15, Table 1). Furthermore, when the reaction was conducted in water (PEG 2000), only trace amount of the desired product was detected. The above studies led to the following optimized protocol: **2a** (0.6 mmol) was added to a solution of **1a** (0.5 mmol) in methanol (5.0 ml) as solvent in presence of piperidine (0.5 mmol)

as base at room temperature. The reaction was stirred for 28 h yielding the desired 1,2,3-triazole-fused indolo-[1,4]diazepine **3a** in 81% isolable yield.

<Insert **Table 1** here>

Subsequent to the optimisation of the reaction conditions, we examined the substrate scope of this metal-free synthetic protocol by employing various *N*-propargyl aldehydes **1** and various substituted phenacylazides **2**. The results obtained from this study (Table 2) suggested the generality of this synthetic method. It was observed that both electron withdrawing and electron-donating substituents on phenacylazide were well tolerated and afforded the fused triazolo-indolo-diazepines. While, the substituted phenacylazide **2** containing electron-donating and neutral groups ( $R^1$ , e.g. methoxy, methyl, amine, hydroxy and acetamide) proceeded smoothly to provide the desired products in good to excellent yields 67-91% (**3a**, **3c**, **3d**, **3f** and **3h**), the electron-withdrawing substituents such as halide functionalities (e.g. F, Cl) exhibited lower efficiency (**3e**, **3k**, 69 and 71% yields). Much to our satisfaction, phenacylazide with 4-Br substitution yielded the triazoloindolodiazepine **3b** in excellent yield. Further, substrates with steric hindrance ( $R^1 = 3$ -acetamido and 4-phenyl) were well tolerated and afforded the products **3f** and **3l** in 81% and 91% yields respectively. Phenacylazide with  $\text{NO}_2$  group at *para* position gave moderate yield and **3g** was obtained in 60% yield. Reaction of 1-(prop-2-yn-1-yl)-1H-indole-2-carbaldehyde **1** with 4-(2-azidoacetyl) benzonitrile **2** failed to give the corresponding 1,2,3-triazole-fused indolodiazepine **3x** under the same reaction conditions. However, when **3c** ( $R^1 = \text{OMe}$ ,) was compared with **3g** ( $R^1 = \text{NO}_2$ ), a strong electron donating effect of the methoxy groups is observed. Consequently, the yield was reduced from 88% to 60%. Furthermore, the C3 substituted indole ( $R = \text{methyl}$ ) gave the corresponding products

(**3i** and **3j**) but the yield was lower than equivalent entries using *N*-propargyl indole-2-carboxaldehyde.

<Insert **Table 2** here>

Further exploration of the scope of the reaction was carried out by replacing indole with pyrrole. The pyrrole fused diazepine tricyclics were obtained in moderate to high yields (58-82%) (Table 2, **3m-w**). Various substituted phenacylazides with both electron-donating groups (such as CH<sub>3</sub>, OMe, acetamido) and electron-withdrawing groups (such as Cl, Br, F, NO<sub>2</sub>) were found to be viable substrates for this reaction, while 3-NO<sub>2</sub> substituted product **3t** was afforded in moderate yield (58%). Increase in the reaction time did not improve the yield even after 35 h. Electron-rich and neutral substrates proceeded in good yields (62-82%). On the other hand, a slight decrease in the yield was observed when methyl substituents were present at the para position of phenacylazide (**3v**, 60%). Furthermore, sterically hindered substrates such as (R<sup>1</sup>= 3-acetamido, 4-phenyl) phenacylazide were also found to be suitable for this transformation **3n** and **3u** (82% and 80% respectively). It should be pointed out that azide-alkyne cycloaddition proceeded without any metal-catalyst at room temperature. Further, when piperidine catalyzed cyclization reaction was explored by replacing indole with imidazole, the reaction did not progress (**3y**).

To demonstrate the synthetic utility of the developed method, a gram-scale reaction was carried out under optimal conditions and the desired product **3l** (2.1 g) was obtained in 78% yield. (Scheme S3, Supporting Information). The structures of the synthesized compounds were confirmed by <sup>1</sup>H NMR, <sup>13</sup>C NMR and HRMS (ESI) spectroscopic techniques and the structure of the compound **3k** was confirmed by single crystal X-ray crystallographic analysis (**figure 2**). The model compound **3a** could be easily confirmed by <sup>1</sup>H NMR spectrum, the CH<sub>2</sub> proton appeared at 5.4 ppm as a singlet and all other aromatic proton found in the range of 6.9–7.9 ppm. The analysis of <sup>13</sup>C NMR spectrum of compound

**3a** showed the one carbonyl signals at 189.0 ppm. The aromatic carbons of **3a** appeared in the range of 138.5–109.3 ppm and aliphatic carbon signal at 37.2 ppm. The  $^1\text{H}$  and  $^{13}\text{C}$  spectra of other derivatives **3b-w** were found to be almost in similar pattern like **3a** for their respective aliphatic and aromatic peaks. The HRMS (ESI) of all the compounds (**3a-w**) showed the characteristic  $[\text{M} + \text{H}]^+$  molecular ion peaks to their respective molecular formula.

<Insert **Figure 2** here>

The plausible reaction mechanism for the piperidinecatalyzed tandem Knoevenagel condensation and azide–alkyne 1,3-dipolar cycloaddition reaction is shown in Scheme 2 [27].

<Insert **Scheme 2** here>

## Biological activity

### *In vitro* cytotoxic activity

The synthesized compounds were submitted to National Cancer Institute (NCI), USA for evaluation of their *in vitro* anticancer activity. The compounds were subjected to preliminary screening at a single dose (single dose study; 10  $\mu\text{M}$ ) against the NCI 60 cell line panel comprising nine human cancer cell types, including, leukemia, non-small cell lung, colon, CNS, melanoma, ovarian, renal, prostate and breast cancer. The compounds were added at a concentration of 10  $\mu\text{M}$  and the cells were incubated for 48 h. End point determinations were made with a protein binding dye, Sulforhodamine B [26]. A perusal of the screening results indicated that the compounds **3b**, **3f** and **3u** are less active against most of the cancer cell lines. Compounds **3a** and **3h** exhibited broad spectrum potent inhibitory activity against all nine subpanels of cancer cell lines tested (Table 3). Among all, compound **3a** exhibited maximum growth inhibition (~94.02%) in MDA-MB-468 cell line compared to other cells. We have tested the cytotoxicity of compound **3a** in normal human keratinocytes (HaCaT

cells), where we observed that compound **3a** showed 35.23% growth inhibition. Hence, molecular mechanistic studies of compound **3a** were performed on MDA-MB-468 cells.

<Insert **Table 3** here>

### Colony forming assay

Antiproliferative activity of compound **3a** was further confirmed by colony forming assay or clonogenic assay. Clonogenic assay is used as an *in vitro* cancer cell survival assay to evaluate the reproductive integrity of cancer cells in a dose-dependent manner. Results from **figure 3** showed that compound **3a** effectively inhibited the clonogenic growth at 0.5  $\mu\text{M}$ . At 2.5  $\mu\text{M}$  concentration, breast cancer cell (MDA-MB-468) colony formation was completely inhibited by compound **3a**.

<Insert **Figure 3** here>

### Cell cycle analysis

Most of the chemotherapeutic compounds exert their growth inhibitory effect by arresting the cell cycle at a specific checkpoint. *In vitro* screening (NCI 60 cell line panel study, table 3) revealed that the compound **3a** showed significant activity against MDA-MB-468 cells. Therefore, we examined the effect of the compound **3a** on cell cycle by using flow cytometry. MDA-MB-468 cells were treated with various concentrations of compound **3a** for 24 h, and stained with propidium iodide, which were analysed by using flow cytometry. The results from **figure 4** indicated that the untreated cells exposed to DMSO showed 4.12% cells in sub G1 phase, whereas compound **3a** treatment resulted in dose dependent accumulation of cells in sub G1 phase. For instance 6.82, 19.33 and 30.04% of cells in sub G1 phase after treatment with 0.5, 1 and 2.5  $\mu\text{M}$  concentrations of compound **3a**. These results demonstrated that treatment of MDA-MB-468 cells with compound **3a** resulted in sub G1 phase cell cycle arrest.

<Insert **Figure 4** here>

### Annexin V binding assay

The apoptosis inducing effect of compound **3a** on MDA-MB-468 cancer cells was further investigated using annexin V-Alexa flour 488/propidium iodide staining assay. MDA-MB-468 cells were treated with 0.5, 1 and 2.5  $\mu\text{M}$  concentration of compound **3a** for 24 h and stained with Annexin V-Alexa flour 488 and propidium iodide. As shown in **figure 5**, the compound **3a** increased the percentage of early apoptotic cells (from 0.02% (ctrl) to 2.66% (0.5  $\mu\text{M}$ ), 7.08% (1.0  $\mu\text{M}$ ) and 66.70% (2.5  $\mu\text{M}$ ) respectively) which indicated that **3a** induced apoptosis of MDA-MB-468 cancer cells in a dose dependent manner.

<Insert **Figure 5** here>

### Mitochondrial dysfunction

Mitochondria are the principal organelles related to energy metabolism and ATP synthesis, and by monitoring the changes in mitochondria membrane potential, mitochondrial function can be examined. Cancer cells exhibit many adaptive responses to drugs, including the changes in mitochondrial function. Mitochondrial dysfunction is involved in apoptotic cell death. The loss of mitochondrial membrane potential (MMP,  $\Delta\Psi\text{m}$ ) is a hallmark of mitochondrial dysfunction. The cationic dye JC-1 was used as the MMP-sensitive probe in which normal polarized mitochondria stains red due to formation of J-aggregates and green colour was observed for depolarized mitochondria of apoptotic cells due to formation of J-monomers. As shown in **figure 6**, MDA-MB-468 cancer cells displayed a distinct red to green colour shift in the presence of different concentrations of **3a**, indicating the loss of MMP compared with the untreated group. The representative JC-1 green signals recorded by flow cytometry are displayed in **figure 6**. These results indicated that mitochondria-mediated pathways participated in the apoptosis of MDA-MB-468 cancer cells caused by compound **3a**.

<Insert **Figure 6** here>

### **DNA-nanodrop method**

DNA-nanodrop experiment indicates the interaction pattern of newly synthesized derivatives with DNA. The quantity and quality of small amount of DNA obtained were determined by Nanodrop UV–vis spectrophotometers. The measurement of changes in absorbance of DNA samples provides the idea of binding of the compounds to DNA. Sharp rise in values is observed when a compound exhibits intercalation into DNA owing to the enhancement in the axial length of DNA helix to adapt the hybrid. Ethidium Bromide (EtBr) is a classical DNA intercalator which corresponds to the increase in absorbance. Groove binding indicates little or no change in terms of absorbance. Compound **3a** with DNA resulted in increase in absorbance in comparison to the control DNA, thereby accounting for the DNA intercalation as shown in (**figure 7A** and **7B**). The graph is plotted between wavelength and absorbance on X and Y axis respectively with doxorubicin, EtBr, compound **3a** and control DNA.

### **Relative viscosity study**

Additionally, we performed relative viscosity studies to determine the DNA intercalation, where we observed that compound **3a** showed more viscosity compared to EtBr and DOX. But the minor groove binder Hoechst-33258 showed more viscosity in comparison with compound **3a**. compounds **3a** showed more viscosity compared to the control DNA in concentration-dependent manner, thereby accounting for the DNA intercalation as shown in (**figure 7C** and **7D**). The graph is plotted between concentration (compound/CTDNA) and viscosity  $(\eta/\eta_0)^{1/3}$  on X and Y axis respectively with EtBr, doxorubicin, and Hoechst 33258 as standards. The viscosity results are well-suited with DNA-nanodrop method and molecular docking studies.

<Insert **Figure 7** here>

## Molecular docking

The biophysical studies have already shown that these compounds possess DNA intercalation properties. Therefore, docking studies were performed to obtain a better insight into the binding mode of the active compounds **3a** to the DNA ternary complex. The coordinates of the protein were obtained from the Protein Data Bank (PDB ID: 1NAB) [28a]. Molecular docking simulations were carried out by using Schrödinger Suite 2017-1 with default settings into DNA duplex and the results were analyzed on the basis of the GLIDE docking score and molecular recognition interactions. All the 3D figures were obtained using Schrödinger Suite 2017-1 [28b].

The docking pose of **3a** shows that the 1,2,3-triazole fused diazepine ring lies in the central part of the DNA intercalation cavity and is stacked between the dC5, dG6 of chain A and dC7, dG8 and dA9 of chain B, while benzoyl substitution of **3a** interacting with dG-B8 nucleotides present in the groove (**figure 8**). The docked compound **3a** was stabilized electronically by  $\pi$ - $\pi$  stacking interactions of the DNA base pairs. The framework has also been stabilized by hydrophobic interactions in the active pocket. Docking studies suggested that 1,2,3-triazole-fused framework have the potential as DNA interacting agents.

*<Insert Figure 8 here>*

## Conclusions

In summary, a facile and efficient method has been developed for the synthesis of fused 1,2,3-triazole indolo- and pyrrolodiazepine derivatives in one pot process. The reaction proceeds via a tandem pathway of an initial Knoevenagel condensation followed by azide-alkyne 1,3-dipolar cycloaddition. The present protocol is compatible with a large variety of substrates, easy to work up, and provides medicinally important polycyclic fused molecules with good to high yields. The synthesized compounds were evaluated for their cytotoxic potential against a panel of 60 cancer cell lines at NCI. The compounds **3a** and **3h** exhibited

potent activity in the preliminary screening. Colony formation assay have shown that at **2.5  $\mu$ M** concentration, breast cancer cell (MDA-MB-468) colony formation was completely inhibited. Further biological studies on compound **3a**, cell cycle arrest at sub G1 phase, apoptosis, mitochondrial dysfunction, DNA-nanodrop experiment, viscosity experiment and molecular docking studies suggested that these compounds possess DNA interacting affinity. Encouragingly, the compound **3a** also exhibited low cytotoxicity on Human keratinocytes, HaCaT.

## Experimental Section

**General Information.**  $^1\text{H}$  and  $^{13}\text{C}$  NMR spectra were recorded in  $\text{CDCl}_3$  or  $\text{DMSO}-d_6$  on a 500 MHz and 125 MHz spectrometer respectively, using tetramethylsilane as the internal standard. Spin multiplicities were described as s (singlet), d (doublet), dd (double doublet), t (triplet), and m (multiplet). Coupling constant ( $J$ ) values were expressed in hertz (Hz). High-resolution mass spectra (HRMS) were recorded on ESI-QTOF mass spectrometer. All the melting points were recorded on micromelting point apparatus and are uncorrected. Thin layer chromatography (TLC) was performed on MERCK precoated silica gel 60<sub>F-254</sub> (0.5 mm) aluminum plates. TLC spot visualization was achieved under UV light. Column chromatography was performed using silica gel 100-200. All starting materials commercially available were used.

### General procedures for the synthesis 1,2,3-Triazole-Fused Indolo- and Pyrrolo[1,4] diazepine Frameworks (3a-x).

To a stirred solution of **1** (0.5 mmol) and **2** (0.6 mmol) in methanol (5 mL) was added 0.50 mmol of piperidine and the resulting reaction mixture was stirred at room temperature. After completion of the reaction (28-30 h), methanol was evaporated in a vacuum and the residue extracted with EtOAc/ Water ( $3 \times 15$  mL). The combined organic layers were dried over anhydrous  $\text{Na}_2\text{SO}_4$  and concentrated at reduced

pressure. The crude reaction mixture was purified by column chromatography on silica gel (100–200 mesh) using ethyl acetate/hexane as an eluent in increasing polarity to yield desired 1,2,3-Triazole-Fused indolo and pyrrolo (1,4 diazepine) frameworks (**3a-w**).

**(4*H*-[1,2,3]triazolo[5',1':3,4][1,4]diazepino[1,7-*a*]indol-12-yl)(phenyl)methanone**

**(3a):** Yield: 81% (132 mg); yellow solid; m.p. 220–221 °C; <sup>1</sup>H NMR (500 MHz, CDCl<sub>3</sub>) δ 7.87 – 7.79 (m, 2H), 7.76 (s, 1H), 7.65 (d, *J* = 8.0 Hz, 1H), 7.62 – 7.56 (m, 1H), 7.47 (t, *J* = 7.8 Hz, 3H), 7.38 (m, 1H), 7.22 (s, 1H), 7.17 (t, *J* = 7.5 Hz, 1H), 6.91 (s, 1H), 5.43 (s, 2H). <sup>13</sup>C NMR (125 MHz, CDCl<sub>3</sub>) δ 189.0, 138.3, 136.4, 133.6, 133.2, 132.7, 131.2, 129.9, 129.5, 128.8, 128.7, 125.2, 122.1, 121.3, 118.6, 111.1, 109.3, 37.2; HRMS (ESI): calcd for C<sub>20</sub>H<sub>15</sub>N<sub>4</sub>O [M + H]<sup>+</sup> 327.1246, found: 327.1248.

**(4*H*-[1,2,3]triazolo[5',1':3,4][1,4]diazepino[1,7-*a*]indol-12-yl)(4-**

**bromophenyl)methanone (3b):** Yield: 82% (198 mg); yellow solid; m.p. 187–189 °C; <sup>1</sup>H NMR (500 MHz, CDCl<sub>3</sub>) δ 7.78 (d, *J* = 8.7 Hz, 1H), 7.70 – 7.65 (m, 3H), 7.62 (d, *J* = 8.6 Hz, 2H), 7.47 (d, *J* = 8.4 Hz, 1H), 7.43 – 7.37 (m, 1H), 7.25 (s, 1H), 7.22 – 7.17 (m, 1H), 6.95 (s, 1H), 5.44 (s, 2H). <sup>13</sup>C NMR (125 MHz, CDCl<sub>3</sub>) δ 187.9, 138.5, 135.3, 133.1, 132.6, 132.1, 131.3, 130.8, 129.4, 128.7, 128.3, 125.4, 122.2, 121.4, 118.8, 111.5, 109.3, 37.2; HRMS (ESI): calcd for C<sub>20</sub>H<sub>14</sub>BrN<sub>4</sub>O [M + H]<sup>+</sup> 405.0351, 407.0331, found: 405.0361, 407.0339.

**4*H*-[1,2,3]triazolo[5',1':3,4][1,4]diazepino[1,7-*a*]indol-12-yl)(4-**

**methoxyphenyl)methanone (3c):** Yield: 88% (187 mg); pale-yellow solid; m.p. 178–180 °C; <sup>1</sup>H NMR (500 MHz, CDCl<sub>3</sub>) δ 7.86 (d, *J* = 8.7 Hz, 2H), 7.78 (s, 1H), 7.65 (d, *J* = 7.9 Hz, 1H), 7.47 (d, *J* = 8.4 Hz, 1H), 7.38 (t, *J* = 7.6 Hz, 1H), 7.20 – 7.14 (m, 2H), 6.96 (d, *J* = 8.8 Hz, 2H), 6.89 (s, 1H), 5.43 (s, 2H), 3.89 (s, 3H). <sup>13</sup>C NMR (125 MHz,

CDCl<sub>3</sub>)  $\delta$  187.6, 164.1, 138.2, 133.3, 132.8, 132.1, 131.2, 130.1, 129.0, 128.3, 125.0, 122.0, 121.2, 117.5, 114.1, 110.5, 109.2, 55.6, 37.2; HRMS (ESI): calcd for C<sub>21</sub>H<sub>17</sub>N<sub>4</sub>O<sub>2</sub> [M + H]<sup>+</sup> 357.1352, found: 357.1357.

**(4*H*-[1,2,3]triazolo[5',1':3,4][1,4]diazepino[1,7-*a*]indol-12-yl)(*p*-tolyl)methanone**

**(3d)**: Yield: 78% (132 mg); pale-yellow; m.p. 234–236 °C; <sup>1</sup>H NMR (500 MHz, CDCl<sub>3</sub>)  $\delta$  7.79 – 7.76 (m, 3H), 7.68 (d, *J* = 8.0 Hz, 1H), 7.49 (d, *J* = 8.4 Hz, 1H), 7.43 – 7.39 (m, 1H), 7.32 – 7.28 (m, 2H), 7.23 (s, 1H), 7.21 (t, *J* = 7.3 Hz, 1H), 6.93 (s, 1H), 5.46 (s, 2H), 2.47 (s, 3H). <sup>13</sup>C NMR (125 MHz, CDCl<sub>3</sub>)  $\delta$  188.6, 144.7, 138.3, 133.7, 133.3, 132.8, 131.1, 130.0, 129.7, 129.5, 128.3, 125.1, 122.1, 121.3, 118.2, 110.8, 109.2, 37.2, 21.8; HRMS (ESI): calcd for C<sub>21</sub>H<sub>17</sub>N<sub>4</sub>O [M + H]<sup>+</sup> 341.1402, found: 341.1409.

**(4*H*-[1,2,3]triazolo[5',1':3,4][1,4]diazepino[1,7-*a*]indol-12-yl)(4-**

**chlorophenyl)methanone (3e)**: Yield: 69% (148 mg); brown solid; m.p. 185–187 °C; <sup>1</sup>H NMR (500 MHz, CDCl<sub>3</sub>)  $\delta$  7.82 – 7.72 (m, 3H), 7.66 (d, *J* = 8.0 Hz, 1H), 7.49 – 7.43 (m, 3H), 7.41 – 7.36 (m, 1H), 7.24 (s, 1H), 7.18 (t, *J* = 7.3 Hz, 1H), 6.94 (s, 1H), 5.43 (s, 2H). <sup>13</sup>C NMR (125 MHz, CDCl<sub>3</sub>)  $\delta$  187.7, 140.1, 138.4, 134.8, 133.1, 132.6, 131.3, 130.8, 129.4, 129.2, 128.3, 125.4, 122.2, 121.4, 118.8, 111.5, 109.3, 37.2; HRMS (ESI): calcd for C<sub>20</sub>H<sub>14</sub>ClN<sub>4</sub>O [M + H]<sup>+</sup> 361.0856, found: 361.0852.

***N*-(3-(4*H*-[1,2,3]triazolo[5',1':3,4][1,4]diazepino[1,7-*a*]indole-12-**

**carbonyl)phenyl)acetamide (3f)**: Yield: 81% (184 mg); yellow solid; m.p. 221–223 °C; <sup>1</sup>H NMR (500 MHz, CDCl<sub>3</sub>)  $\delta$  8.11 (s, 1H), 8.03 (s, 1H), 7.74 (s, 1H), 7.67 – 7.60 (m, 2H), 7.59 – 7.55 (m, 1H), 7.45 (d, *J* = 5.0 Hz, 1H), 7.40 – 7.32 (m, 2H), 7.27 (s, 1H), 7.21 – 7.14 (m, 1H), 6.94 (s, 1H), 5.47 (s, 2H), 2.11 (s, 3H). <sup>13</sup>C NMR (125 MHz, CDCl<sub>3</sub>)  $\delta$  188.7, 169.1, 138.7, 138.4, 136.8, 133.6, 132.6, 131.2, 129.6, 129.4, 128.2,

125.3, 124.6, 124.3, 122.2, 121.3, 120.4, 119.3, 111.4, 109.3, 37.2, 24.5; HRMS (ESI): calcd for  $C_{22}H_{17}N_5NaO_2$   $[M + H]^+$  406.1280, found: 406.1275.

**(4*H*-[1,2,3]triazolo[5',1':3,4][1,4]diazepino[1,7-*a*]indol-12-yl)(4-**

**nitrophenyl)methanone (3g):** Yield: 60% (132 mg); orange solid; m.p. 204–206 °C;  $^1H$  NMR (500 MHz, DMSO- $d_6$ )  $\delta$  8.31 (d,  $J = 8.6$  Hz, 2H), 8.04 (d,  $J = 8.5$  Hz, 2H), 7.96 (s, 1H), 7.86 (d,  $J = 8.4$  Hz, 1H), 7.72 – 7.67 (m, 2H), 7.39 (t,  $J = 10$  Hz, 1H), 7.23 (s, 1H), 7.16 (t,  $J = 10$  Hz, 1H), 5.88 (s, 2H).  $^{13}C$  NMR (125 MHz, DMSO- $d_6$ )  $\delta$  187.9, 150.3, 142.3, 139.1, 135.0, 133.4, 132.1, 130.6, 128.9, 128.1, 125.4, 124.4, 122.3, 121.4, 120.8, 112.4, 111.1, 36.8; HRMS (ESI): calcd for  $C_{20}H_{14}N_5O_3$   $[M + H]^+$  372.1097, found: 372.1105.

**(4*H*-[1,2,3]triazolo[5',1':3,4][1,4]diazepino[1,7-*a*]indol-12-yl)(4-**

**hydroxyphenyl)methanone (3h):** Yield: 82% (140 mg); yellow solid; m.p. 227–229 °C;  $^1H$  NMR (500 MHz, DMSO- $d_6$ )  $\delta$  10.57 (s, 1H), 7.95 (s, 1H), 7.83 (d,  $J = 8.4$  Hz, 1H), 7.75 – 7.69 (m, 2H), 7.66 (d,  $J = 7.9$  Hz, 1H), 7.40 – 7.32 (m, 2H), 7.13 (t,  $J = 7.5$  Hz, 1H), 7.08 (s, 1H), 6.90 – 6.84 (m, 2H), 5.81 (s, 2H).  $^{13}C$  NMR (125 MHz, DMSO- $d_6$ )  $\delta$  187.4, 163.2, 138.5, 134.8, 133.6, 132.5, 131.9, 130.3, 128.1, 127.7, 124.7, 121.9, 121.1, 117.3, 116.1, 110.9, 110.3, 36.8; HRMS (ESI): calcd for  $C_{20}H_{15}N_4O_2$   $[M + H]^+$  343.1195, found: 343.1192.

**(4-hydroxyphenyl)(10-methyl-4*H*-[1,2,3]triazolo[5',1':3,4][1,4]diazepino[1,7-**

**a]indol-12-yl)methanone (3i):** Yield: 71% (125 mg); yellow solid; m.p. 177–179 °C;  $^1H$  NMR (500 MHz, DMSO- $d_6$ )  $\delta$  10.56 (s, 1H), 7.93 (s, 1H), 7.78 (d,  $J = 8.4$  Hz, 1H), 7.72 (d,  $J = 8.7$  Hz, 2H), 7.65 (d,  $J = 7.9$  Hz, 1H), 7.38 – 7.32 (m, 2H), 7.13 (t,  $J = 7.5$  Hz, 1H), 6.87 (d,  $J = 8.7$  Hz, 2H), 5.73 (s, 2H), 2.40 (s, 3H).  $^{13}C$  NMR (125 MHz, DMSO- $d_6$ )  $\delta$  187.5, 163.1, 137.9, 135.0, 132.5, 131.7, 130.3, 129.7, 128.3, 127.9,

125.1, 120.6, 120.3, 118.4, 116.0, 116.0, 110.6, 36.8, 9.2; HRMS (ESI): calcd for  $C_{21}H_{17}N_4O_2$   $[M + H]^+$  357.1352, found: 357.1349.

**(4-bromophenyl)(10-methyl-4*H*-[1,2,3]triazolo[5',1':3,4][1,4]diazepino[1,7-*a*]indol-12-yl)methanone (3j):** Yield: 68% (172 mg); yellow solid; m.p. 186–188 °C;  $^1H$  NMR (500 MHz,  $CDCl_3$ )  $\delta$  7.77 (s, 1H), 7.69 – 7.59 (m, 5H), 7.46 – 7.38 (m, 2H), 7.36 (s, 1H), 7.19 (t,  $J = 7.3$  Hz, 1H), 5.38 (s, 2H), 2.44 (s, 3H).  $^{13}C$  NMR (125 MHz,  $CDCl_3$ )  $\delta$  188.0, 138.0, 135.6, 133.4, 132.1, 131.1, 130.7, 129.7, 128.5, 128.5, 128.4, 125.8, 120.9, 120.8, 120.5, 117.7, 109.1, 37.3, 9.3; HRMS (ESI): calcd for  $C_{21}H_{16}BrN_4O$   $[M + H]^+$  419.0507, 421.0487, found: 419.0515, 421.0493.

**(4*H*-[1,2,3]triazolo[5',1':3,4][1,4]diazepino[1,7-*a*]indol-12-yl)(4-fluorophenyl)methanone (3k):** Yield: 71% (122 mg); yellow solid; m.p. 203–205 °C;  $^1H$  NMR (500 MHz,  $DMSO-d_6$ )  $\delta$  7.96 (s, 1H), 7.93 – 7.88 (m, 2H), 7.84 (d,  $J = 8.4$  Hz, 1H), 7.68 (d,  $J = 8.0$  Hz, 1H), 7.54 (s, 1H), 7.39 – 7.33 (m, 3H), 7.17 – 7.12 (m, 2H), 5.86 (s, 2H).  $^{13}C$  NMR (125MHz,  $DMSO-d_6$ )  $\delta$  187.7, 165.5 (d,  $J_{C-F} = 252.8$  Hz), 138.8, 134.9, 133.5, 133.5, 132.6 (d,  $J_{C-F} = 15.5$  Hz), 132.0, 129.5, 128.1, 125.0, 122.1, 121.3, 119.1, 116.5 (d,  $J_{C-F} = 22.1$  Hz), 111.3, 111.0, 36.8; HRMS (ESI): calcd for  $C_{20}H_{14}FN_4O$   $[M + H]^+$  345.1152, found: 357.1147.

**[1,1'-biphenyl]-4-yl(4*H*-[1,2,3]triazolo[5',1':3,4][1,4]diazepino[1,7-*a*]indol-12-yl)methanone (3l):** Yield: 91% (218 mg); yellow solid; m.p. 247–249 °C;  $^1H$  NMR (500 MHz,  $DMSO-d_6$ )  $\delta$  7.96 (d,  $J = 7.9$  Hz, 1H), 7.93 – 7.89 (m, 2H), 7.87 – 7.81 (m, 3H), 7.78 – 7.74 (m, 2H), 7.68 (d,  $J = 8.0$  Hz, 1H), 7.57 (s, 1H), 7.54 – 7.49 (m, 2H), 7.47 – 7.42 (m, 1H), 7.40 – 7.35 (m, 1H), 7.17 – 7.12 (m, 2H), 5.88 (s, 2H).  $^{13}C$  NMR (125 MHz,  $DMSO-d_6$ )  $\delta$  188.6, 145.4, 139.2, 138.8, 135.6, 134.9, 133.5, 132.0, 130.3, 129.8, 129.6, 129.0, 128.1, 127.5, 125.0, 122.1, 121.2, 118.9, 111.2, 111.0, 36.8; HRMS (ESI): calcd for  $C_{26}H_{19}N_4O$   $[M + H]^+$  403.1559, found: 403.1562.

**phenyl(4*H*-pyrrolo[1,2-*d*][1,2,3]triazolo[1,5-*a*][1,4]diazepin-10-yl)methanone (3m):**

Yield: 79% (132 mg); yellow solid; m.p. 185–187 °C; <sup>1</sup>H NMR (500 MHz, CDCl<sub>3</sub>) δ 7.79 (d, *J* = 7.4 Hz, 2H), 7.67 (s, 1H), 7.61 – 7.54 (m, 1H), 7.50 – 7.43 (m, 2H), 7.16 (s, 1H), 6.94 (s, 1H), 6.57 (dd, *J* = 23.1, 3.4 Hz, 1H), 6.30 (d, *J* = 13.2 Hz, 1H), 5.29 (s, 2H). <sup>13</sup>C NMR (125 MHz, CDCl<sub>3</sub>) δ 188.0, 135.7, 132.8, 132.0, 130.9, 130.7, 128.2, 127.0, 127.0, 126.9, 120.0, 119.0, 111.7, 41.5; HRMS (ESI): calcd for C<sub>16</sub>H<sub>13</sub>N<sub>4</sub>O [M + H]<sup>+</sup> 277.1089, found: 277.1094.

***N*-(3-(4*H*-pyrrolo[1,2-*d*][1,2,3]triazolo[1,5-*a*][1,4]diazepine-10-**

**carbonyl)phenyl)acetamide (3n):** Yield: 82% (162 mg); yellow solid; m.p. 178–180 °C; <sup>1</sup>H NMR (500 MHz, CDCl<sub>3</sub>) δ 8.25 (s, 1H), 7.93 (s, 1H), 7.64 (s, 1H), 7.59 (d, *J* = 8.1 Hz, 1H), 7.49 (d, *J* = 7.6 Hz, 1H), 7.30 (t, *J* = 7.9 Hz, 1H), 7.20 (s, 1H), 6.93 (s, 1H), 6.61 (d, *J* = 2.7 Hz, 1H), 6.33 – 6.27 (m, 1H), 5.28 (s, 2H), 2.08 (s, 3H). <sup>13</sup>C NMR (125 MHz, CDCl<sub>3</sub>) δ 188.9, 169.0, 138.6, 137.2, 133.3, 130.8, 129.3, 127.0, 127.0, 124.5, 124.1, 120.4, 120.3, 119.0, 111.6, 41.5, 24.5; HRMS (ESI): calcd for C<sub>18</sub>H<sub>16</sub>N<sub>5</sub>O<sub>2</sub> [M + H]<sup>+</sup> 334.1304, found: 334.1301.

**(3-aminophenyl)(4*H*-pyrrolo[1,2-*d*][1,2,3]triazolo[1,5-*a*][1,4]diazepin-10-**

**yl)methanone (3o):** Yield: 82% (162 mg); pale-yellow solid; m.p. 172–174 °C; <sup>1</sup>H NMR (500 MHz, CDCl<sub>3</sub>) δ 7.69 (s, 1H), 7.29 (s, 1H), 7.23 (s, 1H), 7.15 (s, 1H), 7.10 (d, *J* = 6.2 Hz, 1H), 6.97 – 6.87 (m, 2H), 6.61 (s, 1H), 6.34 (s, 1H), 5.27 (s, 2H). <sup>13</sup>C NMR (125 MHz, CDCl<sub>3</sub>) δ 194.2, 142.4, 138.2, 135.6, 135.5, 134.1, 132.1, 131.8, 131.6, 124.8, 124.6, 123.9, 123.1, 120.3, 116.0, 45.9; HRMS (ESI): calcd for C<sub>16</sub>H<sub>14</sub>N<sub>5</sub>O [M + H]<sup>+</sup> 292.1198, found: 334.1204.

**(4-chlorophenyl)(4*H*-pyrrolo[1,2-*d*][1,2,3]triazolo[1,5-*a*][1,4]diazepin-10-**

**yl)methanone (3p):** Yield: 63% (117 mg); brown solid; m.p. 182–184 °C; <sup>1</sup>H NMR (500 MHz, CDCl<sub>3</sub>) δ 7.76 – 7.65 (m, 3H), 7.47 – 7.38 (m, 2H), 7.16 (s, 1H), 6.95 (s, 1H), 6.69 – 6.58 (m, 1H), 6.35 – 6.33 (m, 1H), 5.28 (s, 2H). <sup>13</sup>C NMR (125 MHz,

CDCl<sub>3</sub>)  $\delta$  187.8, 139.6, 135.2, 132.8, 130.9, 130.6, 129.0, 127.0, 126.9, 119.9, 119.0, 111.7, 41.5; HRMS (ESI): calcd for C<sub>16</sub>H<sub>11</sub>ClN<sub>4</sub>NaO [M + Na]<sup>+</sup> 333.0519, found: 333.0516.

**(4-methoxyphenyl)(4*H*-pyrrolo[1,2-*d*][1,2,3]triazolo[1,5-*a*][1,4]diazepin-10-**

**yl)methanone (3q):** Yield: 82% (150 mg); yellow solid; m.p. 168–170 °C; <sup>1</sup>H NMR (500 MHz, CDCl<sub>3</sub>)  $\delta$  7.82 – 7.75 (m, 2H), 7.65 (s, 1H), 7.06 (s, 1H), 6.94 – 6.89 (m, 3H), 6.55 (dd, *J* = 3.8, 1.4 Hz, 1H), 6.29 (dd, *J* = 3.8, 2.7 Hz, 1H), 5.24 (s, 2H), 3.86 (s, 3H). <sup>13</sup>C NMR (125 MHz, CDCl<sub>3</sub>)  $\delta$  187.8, 163.8, 132.9, 131.9, 130.8, 129.3, 127.5, 127.0, 126.3, 118.7, 117.9, 114.0, 111.3, 55.6, 41.5; HRMS (ESI): calcd for C<sub>17</sub>H<sub>15</sub>N<sub>4</sub>O<sub>2</sub> [M + H]<sup>+</sup> 307.1195, found: 307.1210.

**(4-bromophenyl)(4*H*-pyrrolo[1,2-*d*][1,2,3]triazolo[1,5-*a*][1,4]diazepin-10-**

**yl)methanone (3r):** Yield: 70% (148 mg); yellow solid; m.p. 167–169 °C; <sup>1</sup>H NMR (500 MHz, CDCl<sub>3</sub>)  $\delta$  7.68 (s, 1H), 7.61 (dd, *J* = 19.7, 8.6 Hz, 4H), 7.16 (s, 1H), 6.94 (s, 1H), 6.62 (dd, *J* = 3.8, 1.3 Hz, 1H), 6.37 – 6.31 (m, 1H), 5.27 (s, 2H). <sup>13</sup>C NMR (125 MHz, CDCl<sub>3</sub>)  $\delta$  187.9, 135.7, 132.7, 132.0, 130.9, 130.7, 128.2, 127.0, 126.9, 119.8, 118.9, 111.7, 41.5; HRMS (ESI): calcd for C<sub>16</sub>H<sub>12</sub>BrN<sub>4</sub>O [M + H]<sup>+</sup> 355.0194, 357.0174, found: 355.0198, 357.0181.

**(4-hydroxyphenyl)(4*H*-pyrrolo[1,2-*d*][1,2,3]triazolo[1,5-*a*][1,4]diazepin-10-**

**yl)methanone (3s):** Yield: 76% (132 mg); grey solid; m.p. 271–273 °C; <sup>1</sup>H NMR (500 MHz, DMSO-*d*<sub>6</sub>)  $\delta$  10.48 (s, 1H), 7.85 (s, 1H), 7.64 (d, *J* = 8.6 Hz, 2H), 7.22 (m, 2H), 6.83 (d, *J* = 8.7 Hz, 2H), 6.68 (dd, *J* = 3.8, 1.5 Hz, 1H), 6.28 (dd, *J* = 3.7, 2.6 Hz, 1H), 5.57 (s, 2H). <sup>13</sup>C NMR (125 MHz, DMSO-*d*<sub>6</sub>)  $\delta$  187.5, 162.7, 134.3, 132.3, 131.4, 128.1, 127.6, 127.4, 127.1, 118.6, 118.1, 115.9, 111.0, 40.6; HRMS (ESI): calcd for C<sub>16</sub>H<sub>13</sub>N<sub>4</sub>O<sub>2</sub> [M + H]<sup>+</sup> 293.1039, found: 293.1043.

**(3-nitrophenyl)(4*H*-pyrrolo[1,2-*d*][1,2,3]triazolo[1,5-*a*][1,4]diazepin-10-**

**yl)methanone (3t):** Yield: 58% (112 mg); yellow solid; m.p. 199–201 °C; <sup>1</sup>H NMR (500 MHz, CDCl<sub>3</sub>) δ 8.46 – 8.37 (m, 2H), 8.06 (d, *J* = 6.7 Hz, 1H), 7.76 – 7.61 (m, 2H), 7.32 (s, 1H), 7.01 (s, 1H), 6.70 (s, 1H), 6.33 (s, 1H), 5.34 (s, 2H). <sup>13</sup>C NMR (125 MHz, CDCl<sub>3</sub>) δ 186.5, 148.1, 138.7, 134.5, 132.6, 131.2, 130.0, 127.8, 127.1, 126.0, 123.7, 120.9, 120.0, 112.1, 41.6; HRMS (ESI): calcd for C<sub>16</sub>H<sub>12</sub>N<sub>5</sub>O<sub>3</sub> [M + H]<sup>+</sup> 322.0940, found: 322.0949.

**[1,1'-biphenyl]-4-yl(4*H*-pyrrolo[1,2-*d*][1,2,3]triazolo[1,5-*a*][1,4]diazepin-10-**

**yl)methanone (3u):** Yield: 80% (168 mg); pale-yellow solid; m.p. 192–194 °C; <sup>1</sup>H NMR (500 MHz, DMSO-*d*<sub>6</sub>) δ 7.87 (s, 1H), 7.85 – 7.81 (m, 2H), 7.79 (d, *J* = 8.5 Hz, 2H), 7.77 – 7.72 (m, 2H), 7.53 – (m, 2H), 7.43 (t, *J* = 7.3 Hz, 1H), 7.40 (s, 1H), 7.30 – 7.27 (m, 1H), 6.76 (dd, *J* = 3.8, 1.5 Hz, 1H), 6.32 (dd, *J* = 3.8, 2.6 Hz, 1H), 5.64 (s, 2H). <sup>13</sup>C NMR (125 MHz, DMSO-*d*<sub>6</sub>) δ 188.6, 144.9, 139.3, 136.1, 134.4, 131.6, 130.1, 129.6, 128.9, 128.3, 127.5, 127.3, 127.2, 126.9, 120.1, 119.1, 111.3, 40.6; HRMS (ESI): calcd for C<sub>22</sub>H<sub>17</sub>N<sub>4</sub>O [M + H]<sup>+</sup> 353.1402, found: 343.1398.

**(4*H*-pyrrolo[1,2-*d*][1,2,3]triazolo[1,5-*a*][1,4]diazepin-10-yl)(*p*-tolyl)methanone**

**(3v):** Yield: 60% (105 mg); brown solid; m.p. 181–183 °C; <sup>1</sup>H NMR (500 MHz, CDCl<sub>3</sub>) δ 7.65 – 7.58 (m, 3H), 7.18 (m, 2H), 7.05 (s, 1H), 6.87 – 6.82 (m, 1H), 6.51 (dd, *J* = 3.8, 1.4 Hz, 1H), 6.25 (dd, *J* = 3.8, 2.7 Hz, 1H), 5.19 (s, 2H), 2.35 (s, 3H). <sup>13</sup>C NMR (125 MHz, CDCl<sub>3</sub>) δ 189.0, 144.3, 134.2, 133.0, 130.9, 129.7, 129.5, 127.7, 127.2, 126.6, 119.5, 118.3, 111.6, 41.6, 21.9; HRMS (ESI): calcd for C<sub>17</sub>H<sub>15</sub>N<sub>4</sub>O [M + H]<sup>+</sup> 291.1246, found: 291.1229.

**(4-fluorophenyl)(4*H*-pyrrolo[1,2-*d*][1,2,3]triazolo[1,5-*a*][1,4]diazepin-10-yl)methanone**

**(3w):** Yield: 66% (116 mg); yellow solid; m.p. 165–167 °C; <sup>1</sup>H NMR (500 MHz, DMSO-*d*<sub>6</sub>) δ 7.85 (s, 1H), 7.83 – 7.79 (m, 2H), 7.37 (s, 1H), 7.33 – 7.29 (m, 2H), 7.29 – 7.26 (m, 1H),

6.75 (dd,  $J = 3.8, 1.5$  Hz, 1H), 6.31 (dd,  $J = 3.7, 2.6$  Hz, 1H), 5.61 (s, 2H).  $^{13}\text{C}$  NMR (125 MHz, DMSO- $d_6$ )  $\delta$  187.7, 165.2 (d,  $J_{\text{C-F}} = 251.9$  Hz), 134.4, 134.0 (d,  $J_{\text{C-F}} = 2.8$  Hz), 132.3 (d,  $J_{\text{C-F}} = 9.4$  Hz), 131.5, 128.4, 127.2, 126.6, 120.3, 119.2, 116.3, (d,  $J_{\text{C-F}} = 22.1$  Hz), 111.3, 40.6; HRMS (ESI): calcd for  $\text{C}_{16}\text{H}_{12}\text{FN}_4\text{O}$   $[\text{M} + \text{H}]^+$  295.0995, found: 295.0989.

## Biology

### *In vitro* cytotoxic (NCI-screening)

The synthesized compounds were evaluated to National Cancer Institute (NCI), USA for evaluation of their *in vitro* anticancer activity. The compounds were subjected to preliminary screening at a single dose (single dose study; 10  $\mu\text{M}$ ) for their growth inhibition effects against the NCI 60 cell line panel comprising nine human cancer cell types, including, leukemia, non-small cell lung, colon, CNS, melanoma, ovarian, renal, prostate and breast cancer. The compounds were added at a concentration of 10  $\mu\text{M}$  and the cells were incubated for 48 h. Compounds were submitted to Developmental Therapeutics Program (DTP) at National Cancer Institute (NCI) for anti-cancer on single dose basis.

### Determination of growth inhibition on normal cell (Human keratinocytes, HaCaT)

Cells (5000 cells per well) were seeded in 96-well plate and allow to grow for overnight. After attaching the cells and before going to treatment (day 0), the absorbance was taken by adding 3-(4,5-dimethylthiazol-2-yl)-2,5-diphenyl tetrazolium bromide (MTT) (0.5 mg/ml) reagent to a few wells. After 48 h of incubation, MTT was added, and the cells were incubated for 4 h at 37 °C in  $\text{CO}_2$  incubator. Then the cells were washed with and PBS and formazan crystals were dissolved in DMSO and the absorbance was taken at 570 nm using multimode plate reader (Spectra Max, M4 Molecular devices, USA). The day 0 absorbance was subtracted from the 48 h reading to determine the percentage growth inhibition.

### Colony formation assay

MDA-MB-468 cancer cells were seeded into 12-well culture plate at a single cell density of 250 cells/well. After cells adhered to the culture well plate, cells were treated with different concentrations of **3a** (0.5, 1 and 2.5  $\mu\text{M}$ ) for 24 hrs. Post incubation, media was discarded and the cells were maintained in fresh medium, cells were washed with PBS and incubated for next 12 days at 37 °C. After 12 days, the so called colonies were stained with 1% crystal violet for 3 h and washed with PBS. Then, the Plates were photographed and colonies were counted using Vilber Fusion Fx software (Vilber Lourmat, France). The results were represented as total colony number vs. concentration.

### Cell cycle analysis

To perform cell cycle analysis assay, MDA-MB-468 cancer cells (1 X 10<sup>6</sup> cells/well) in 6 well plate were treated with 0.5, 1 and 2.5  $\mu\text{M}$  of compound **3a** for 24 hrs. cells were harvested by trypsinisation, washed with PBS and fixed with ethanol (70 %) at 4 °C for 30 min. After fixation, cells were again washed with PBS (400  $\mu\text{L}$ ) and stained with propidium iodide staining buffer for 30 min in dark at room temperature. Then, the samples were analyzed for propidium iodide fluorescence by flow cytometry using BD Accuri C6 flow-cytometer.

### AnnexinV/Propidium iodide staining assay

MDA-MB-468 cells were plated at a density of 5 x 10<sup>3</sup> cells in a 12-well culture plates and allowed to grow for 24 h. Then cells were treated with **3a** at concentration of 0.5, 1 and 2.5  $\mu\text{M}$ . After 48 hrs, cells were collected by trypsinisation. The collected cells were rinsed with ice-cold PBS (two times), then incubated with 200  $\mu\text{L}$  1X binding buffer containing 5  $\mu\text{L}$  Annexin V-FITC, and then in 300  $\mu\text{L}$  1X binding buffer containing 5  $\mu\text{L}$  Propidium iodide

(PI) in the dark for 5 min at room temperature and incubate for 15 min. After incubation, cells were analysed for percentage of apoptosis using BD-C6 accuri flow-cytometer.

### **Assay of mitochondrial membrane potential ( $\Delta\psi_m$ )**

The mitochondrial- specific cationic dye JC-1 (Invitrogen, USA), which undergoes potential-dependent accumulation mitochondria, was used to detect mitochondrial membrane potential. Briefly, MDA-MB-468 cells were plated at density of  $2 \times 10^5$  cells/well in a 12-well plate. Then cells were treated with **3a** at concentration of 0.5, 1 and 2.5  $\mu\text{M}$  for 48 hrs. After 48 hrs cells were incubated with 2  $\mu\text{M}$  JC-1 in the dark for 30 min at room temperature. After incubation, cells were observed by flow cytometry for the quantitative analysis of  $\Delta\psi_m$ . At least 10,000 events per sample were recorded.

### **DNA-nanodrop method**

DNA intercalation is determined by nanodrop spectrophotometric analysis. The intercalating agents decrease the absorption and increase the wavelengths [29]. In our experiment, we incubated the 50  $\mu\text{M}$  of calf thymus DNA (Sigma-Aldrich, USA) with compound **3a**, Ethidium bromide (EtBr) and Doxorubicin (DOX) for 10 min at 1  $\mu\text{M}$  concentration. Later, the TAE buffer used as blank and absorbance and concentrations were determined by NanoDrop™ 2000/2000c Spectrophotometer (Thermo fisher scientific, USA).

### **DNA binding affinity studies**

Relative studies were determined by Ostwald viscometer. The titrations were conducted for **3a**, DOX, EtBr and Hoechst-33258 at 1.0  $\mu\text{M}$  while and they are added to CT-DNA solution (50  $\mu\text{M}$ ) and exposed to viscometer. Here, the DNA solution was prepared in 100 mM Tris-HCl (pH 7.0). Data were represented as  $(\eta/\eta_0)^{1/3}$  versus the ratio of the concentration of the

compound **3a**, DOX, EtBr and Hoechst-33258 to CT-DNA, where  $\eta$  is the viscosity of CT-DNA in the presence of intercalating agents and  $\eta_0$  is the viscosity of CT-DNA alone.

## **Molecular modelling**

### **Protein preparation and Grid generation**

The 3D coordinates of the disaccharide anthracycline with DNA hexamer d(CGATCG) was obtained from Protein Data Bank (PDB ID code: PDB 1NAB). The PDB protein-ligand structures were processed with the Protein Preparation Wizard in the Schrödinger suite. The protein structure integrity was checked and adjusted, and missing residues and loop segments near the active site were added using Prime. A 3D box was generated around each ligand to enclose the entire vicinity of active site. The receptor grid was prepared with the help of OPLS\_2005 force field. The grid center was set to be the centroid of the co-crystallized ligand, and the cubic grid had a size of 20 Å.

### **Ligand preparation**

3D structures were generated by Schrödinger suite. Schrödinger's LigPrep program was used to generate different conformations of ligands.

### **Molecular docking**

Molecular docking studies were performed by using a GLIDE docking module of Schrödinger suite 2017-1. For the validation of docking protocol, the cocrystallized ligand (disaccharide anthracycline) was subjected to re-docking into DNA (PDB code: 1NAB) using GLIDE, then the prepared ligands were docked into the generated receptor grids using Glide SP docking precision. The results were analyzed on the basis of the GLIDE docking score and molecular recognition interactions. The 3D images were generated using Schrödinger Suite 2017-1[28].

## Statistical analysis

Biological assays results were expressed as mean  $\pm$  SD, and n refers to the number of sample repeats. The statistical differences between the means were determined by one-way ANOVA then Tukey's multiple comparison tests with Prism software (version 6.01; GraphPad, USA).  $p < 0.05$  was considered to be statistically significant.

## Acknowledgments

We are grateful to DoP, Ministry of Chemicals & Fertilizers, Govt. of India, New Delhi, for the award of NIPER fellowship. We are thankful to Dr. Mohammed Nayel, Developmental Therapeutics Program (DTP), National Cancer Institute (NCI), Chemotherapeutic Agents Repository, Fisher BioServices, Rockville, MD, USA, and the team for *in-vitro* anticancer screening of the compounds. We thank N. Jagadeesh Babu, Centre for X-ray Crystallography, IICT, Hyderabad for carrying out X-ray Crystallography studies.

## References

- [1] F. Bray, J. Ferlay, I. Soerjomataram, R.L. Siegel, L.A. Torre, A. Jemal, Global cancer statistics 2018: GLOBOCAN estimates of incidence and mortality worldwide for 36 cancers in 185 countries, *CA Cancer J Clin.*, 68 (2018) 394-424.
- [2] M. Hranjec, M. Kralj, I. Piantanida, M. Sedić, L. Šuman, K. Pavelić, G. Karminski-Zamola, Novel cyano-and amidino-substituted derivatives of styryl-2-benzimidazoles and benzimidazo [1, 2-*a*] quinolines. Synthesis, photochemical synthesis, DNA binding, and antitumor evaluation, part 3, *J. Med. Chem.*, 50 (2007) 5696-5711.

- [3] M.D. Tomczyk, K.Z. Walczak, 1, 8-Naphthalimide based DNA intercalators and anticancer agents. A systematic review from 2007 to 2017, *Eur. J. Med. Chem.*, 159 (2018) 393-422.
- [4] A. Rescifina, C. Zagni, M.G. Varrica, V. Pistara, A. Corsaro, Recent advances in small organic molecules as DNA intercalating agents: Synthesis, activity, and modeling, *Eur. J. Med. Chem.*, 74 (2014) 95-115.
- [5] (a) Z. Wang, F. Song, Y. Zhao, Y. Huang, L. Yang, D. Zhao, J. Lan, J. You, Elements of Regiocontrol in the Direct Heteroarylation of Indoles/Pyrroles: Synthesis of Bi-and Fused Polycyclic Heteroarenes by Twofold or Tandem Fourfold C–H Activation, *Chem. Eur. J.*, 18 (2012) 16616-16620; (b) G. Abbiati, A. Casoni, V. Canevari, D. Nava, E. Rossi, TiCl<sub>4</sub>/t-BuNH<sub>2</sub>-Promoted Hydroamination/Annulation of  $\delta$ -Keto-acetylenes: Synthesis of Novel Pyrrolo [1, 2-*a*] indol-2-carbaldehydes, *Org. Lett.*, 8 (2006) 4839-4842.
- [6] (a) Q.-Q. Liu, K. Lu, H.-M. Zhu, S.-L. Kong, J.-M. Yuan, G.-H. Zhang, N.-Y. Chen, C.-X. Gu, C.-X. Pan, D.-L. Mo, Identification of 3-(benzazol-2-yl) quinoxaline derivatives as potent anticancer compounds: Privileged structure-based design, synthesis, and bioactive evaluation in vitro and in vivo, *Eur. J. Med. Chem.*, 165 (2019) 293-308; (b) H. Zhao, J. Dietrich, Privileged scaffolds in lead generation, *Expert Opin. Drug Discov.*, 10 (2015) 781-790.
- [7] (a) L. Keller, S. Beaumont, J.-M. Liu, S. Thoret, J.S. Bignon, J. Wdzieczak-Bakala, P. Dauban, R.H. Dodd, New C5-alkylated indolobenzazepinones acting as inhibitors of tubulin polymerization: cytotoxic and antitumor activities, *J. Med. Chem.*, 51 (2008) 3414-3421; (b) J. Zhu, H. Xie, Z. Chen, S. Li, Y. Wu, Synthesis of 6-trifluoromethylindolo [1, 2-*c*] quinazolines and related heterocycles using N-(2-iodophenyl) trifluoroacetimidoyl chlorides as starting material via C–H bond functionalization, *Chem. Commun.*, 47 (2011) 1512-1514;

(c)A. Brancale, R. Silvestri, Indole, a core nucleus for potent inhibitors of tubulin polymerization, *Med. Res. Rev.*, 27 (2007) 209-238.

[8] (a) N. Sudhapriya, A. Nandakumar, Y. Arun, P. Perumal, C. Balachandran, N. Emi, An expedient route to highly diversified [1, 2, 3] triazolo [1, 5-a][1, 4] benzodiazepines and their evaluation for antimicrobial, antiproliferative and in silico studies, *RSC Adv.*, 5 (2015) 66260-66270; (b) X. Zhang, S. Zhi, W. Wang, S. Liu, J.P. Jasinski, W. Zhang, A pot-economical and diastereoselective synthesis involving catalyst-free click reaction for fused-triazolobenzodiazepines, *Green Chem.*, 18 (2016) 2642-2646.

[9] G. Beke, J. Éles, A. Boros, S. Farkas, G. M. Keseru, Indole derivatives PCT WO 2016/166684 A1, October 20, 2016.

[10] A.J. Molinari, E.J. Trybulski, J. Bagli, S. Croce, J. Considine, J. Qi, K. Ali, W. DeMaio, L. Lihotz, D. Cochran, Identification and synthesis of major metabolites of Vasopressin V2-receptor agonist WAY-151932, and antagonist, Lixivaptan, *Bioorg. Med. Chem. Lett.*, 17 (2007) 5796-5800.

[11] (a) L. Shen, N. Xie, B. Yang, Y. Hu, Y. Zhang, Design and total synthesis of Mannich derivatives of marine natural product lamellarin D as cytotoxic agents, *Eur. J. Med. Chem.*, 85 (2014) 807-817; (b) X. Zheng, T.W. Hudyma, S.W. Martin, C. Bergstrom, M. Ding, F. He, J. Romine, M. A. Poss, J. F. Kadow, C.-H. Chang, Syntheses and initial evaluation of a series of indolo-fused heterocyclic inhibitors of the polymerase enzyme (NS5B) of the hepatitis C virus, *Bioorg. Med. Chem. Lett.*, 21 (2011) 2925-2929; (c) V.N. Danilenko, A.Y. Simonov, S.A. Lakatosh, M.H. Kubbutat, F. Totzke, C. Schächtele, S.M. Elizarov, O.B. Bekker, S.S. Printsevskaya, Y.N. Luzikov, Search for inhibitors of bacterial and human protein kinases among derivatives of diazepines [1, 4] annelated with maleimide and indole cycles, *J. Med. Chem.*, 51 (2008) 7731-7736; (d) A. Putey, G. Fournet, O. Lozach, L. Perrin, L. Meijer, B. Joseph, Synthesis and biological evaluation of tetrahydro [1, 4] diazepino [1, 2-

a] indol-1-ones as cyclin-dependent kinase inhibitors, *Eur. J. Med. Chem.*, 83 (2014) 617-629; (e) M. Ding, F. He, M.A. Poss, K.L. Rigat, Y.-K. Wang, S.B. Roberts, D. Qiu, R.A. Fridell, M. Gao, R.G. Gentles, The synthesis of novel heteroaryl-fused 7, 8, 9, 10-tetrahydro-6 H-azepino [1, 2-*a*] indoles, 4-oxo-2, 3-dihydro-1 H-[1, 4] diazepino [1, 7-*a*] indoles and 1, 2, 4, 5-tetrahydro-[1, 4] oxazepino [4, 5-*a*] indoles. Effective inhibitors of HCV NS5B polymerase, *Org. Biomol. Chem.*, 9 (2011) 6654-6662.

[12] (a) R. Alvarez, S. Velazquez, A. San-Felix, S. Aquaro, E.D. Clercq, C.-F. Perno, A. Karlsson, J. Balzarini, M.J. Camarasa, 1, 2, 3-Triazole-[2, 5-Bis-O-(tert-butyldimethylsilyl)-beta.-D-ribofuranosyl]-3'-spiro-5''-(4''-amino-1'', 2''-oxathiole 2'', 2''-dioxide)(TSAO) Analogs: Synthesis and Anti-HIV-1 Activity, *J. Med. Chem.*, 37 (1994) 4185-4194; (b) D.K. Mohapatra, P.K. Maity, M. Shabab, M. Khan, Click chemistry based rapid one-pot synthesis and evaluation for protease inhibition of new tetracyclic triazole fused benzodiazepine derivatives, *Bioorg. Med. Chem. Lett.*, 19 (2009) 5241-5245.

[13] P. Filippakopoulos, J. Qi, S. Picaud, Y. Shen, W.B. Smith, O. Fedorov, E.M. Morse, T. Keates, T.T. Hickman, I. Felletar, Selective inhibition of BET bromodomains, *Nature*, 468 (2010) 1067.

[14] Y. Zhao, C.-Y. Yang, S. Wang, The making of I-BET762, a BET bromodomain inhibitor now in clinical development, *J. Med. Chem.*, 56 (2013) 7498-7500.

[15] S.M. Ali, M.A. Ashwell, E. Kelleher, S. Koerner, J.-M. Lapierre, J.S. Link, Y. Liu, M. Moussa, R. Palma, M. Tandon, Substituted benzo-pyrido-triazolo-diazepine compounds,, US Pat. 8,541,407 B2, (2013).

[16] (a) D. Antonow, D.E. Thurston, Synthesis of DNA-interactive pyrrolo[2, 1-*c*][1, 4]benzodiazepines (PBDs), *Chem. Rev.*, 111 (2010) 2815-2864; (b) D.E. Thurston, D.S. Bose, P.W. Howard, T.C. Jenkins, A. Leoni, P.G. Baraldi, A. Guiotto, B. Cacciari, L.R.

Kelland, M.-P. Foloppe, Effect of A-ring modifications on the DNA-binding behavior and cytotoxicity of pyrrolo [2, 1-*c*][1, 4] benzodiazepines, *J. Med. Chem.*, 42 (1999) 1951-1964.

[17] (a) P.G. Baraldi, A. Leoni, B. Cacciari, S. Manfredini, D. Simoni, M. Bergomi, E. Menta, S. Spinelli, Synthesis and antitumor activity of a new class of Pyrazolo [4, 3-*e*] pyrrolo [1, 2-*a*][1, 4]diazepinone analogs of pyrrolo[1, 4][2, 1-*c*]benzodiazepines, *J. Med. Chem.*, 37 (1994) 4329-4337; (b) A. Kamal, G. Ramesh, N. Laxman, P. Ramulu, O. Srinivas, K. Neelima, A.K. Kondapi, V. Sreenu, H. Nagarajaram, Design, synthesis, and evaluation of new noncross-linking pyrrolobenzodiazepine dimers with efficient DNA binding ability and potent antitumor activity, *J. Med. Chem.*, 45 (2002) 4679-4688.

[18] (a) N. Das Adhikary, P. Chattopadhyay, Design and synthesis of 1, 2, 3-triazole-fused chiral medium-ring benzo-heterocycles, scaffolds mimicking benzolactams, *J. Org. Chem.*, 77 (2012) 5399-5405; (b) K.R. Senwar, P. Sharma, T.S. Reddy, M.K. Jeengar, V.L. Nayak, V. Naidu, A. Kamal, N. Shankaraiah, Spirooxindole-derived morpholine-fused-1,2,3-triazoles: Design, synthesis, cytotoxicity and apoptosis inducing studies, *Eur. J. Med. Chem.*, 102 (2015) 413-424; (c) M.J. Soble, R.T. Dorr, P. Plezia, S. Breckenridge, Dose-dependent skin ulcers in mice treated with DNA binding antitumor antibiotics, *Cancer Chemother. Pharmacol.*, 20 (1987) 33-36.

[19] For the synthesis of related indolo and pyrrolo-diazepine see: (a) T.U. Thikekar, C.M. Sun, Palladium-Catalyzed Regioselective Synthesis of 1,2-Fused Indole-Diazepines via [5+2] Annulation of *o*-Indoloanilines with Alkynes, *Adv. Syn. Catal.*, 359 (2017) 3388-3396; (b) M.K. Hussain, M.I. Ansari, R. Kant, K. Hajela, Tandem C-2 Functionalization–Intramolecular Azide–Alkyne 1,3-Dipolar Cycloaddition Reaction: A Convenient Route to Highly Diversified 9*H*-Benzo[*b*]pyrrolo [1,2-*g*][1,2,3] triazolo [1,5-*d*][1,4] diazepines, *Org. Lett.*, 16 (2013) 560-563; (c) Y. He, M. Lin, Z. Li, X. Liang, G. Li, J.C. Antilla, Direct

synthesis of chiral 1,2,3,4-tetrahydropyrrolo [1,2-*a*] pyrazines via a catalytic asymmetric intramolecular aza-Friedel–Crafts reaction, *Org. Lett.*, 13 (2011) 4490-4493; (d) C.-X. Zhuo, X. Zhang, S.-L. You, Enantioselective Synthesis of Pyrrole-Fused Piperazine and Piperazinone Derivatives via Ir-Catalyzed Asymmetric Allylic Amination, *ACS Catal.*, 6 (2016) 5307-5310.

[20] Y. Ohta, H. Chiba, S. Oishi, N. Fujii, H. Ohno, Concise Synthesis of Indole-Fused 1,4-Diazepines through Copper (I)-Catalyzed Domino Three-Component Coupling–Cyclization–N-Arylation under Microwave Irradiation, *Org. Lett.*, 10 (2008) 3535-3538.

[21] S. Basceken, S. Kaya, M. Balci, Intramolecular gold-catalyzed and NaH-supported cyclization reactions of N-propargyl indole derivatives with pyrazole and pyrrole rings: synthesis of pyrazolodiazepinoindole, pyrazolopyrazinoindole, and pyrrolopyrazinoindole, *J. Org. Chem.*, 80 (2015) 12552-12561.

[22] H. H. Nguyen, T. A. Palazzo, M.J. Kurth, Facile one-pot assembly of imidazotriazolobenzodiazepines via indium (III)-catalyzed multicomponent reactions, *Org. Lett.*, 15 (2013) 4492-4495.

[23] (a) G. Silveira-Dorta, S. Jana, L. Borkova, J. Thomas, W. Dehaen, Straightforward synthesis of enantiomerically pure 1, 2, 3-triazoles derived from amino esters, *Org. Biomol. Chem.*, 16 (2018) 3168-3176; (b) Z. Chen, Q. Yan, H. Yi, Z. Liu, A. Lei, Y. Zhang, Efficient Synthesis of 1,2,3-Triazoles by Copper-Mediated C–N and N–N Bond Formation Starting From N-Tosylhydrazones and Amines, *Chem. Eur. J.*, 20 (2014) 13692-13697.

[24] Y. Zhou, P.V. Murphy, New Access to 1-Deoxynojirimycin Derivatives via Azide–Alkene Cycloaddition, *Org. Lett.*, 10 (2008) 3777-3780.

[25] J. Gour, S. Gatadi, A. Nagarsenkar, B.N. Babu, Y. Madhavi, S. Nanduri, Synthesis of Indolo[1,2-*b*]isoquinoline Derivatives by Lewis Acid-Catalyzed Intramolecular Friedel–Crafts Alkylation Reaction, *Eur. J. Org. Chem.*, 22 (2018) 2817-2821.

- [26] (a) A. Monks, D. Scudiero, P. Skehan, R. Shoemaker, K. Paull, D. Vistica, C. Hose, J. Langley, P. Cronise, A. Vaigro-Wolff, Feasibility of a high-flux anticancer drug screen using a diverse panel of cultured human tumor cell lines, *J. Natl. Cancer Inst.*, 83 (1991) 757-766; (b) M.R. Grever, S.A. Schepartz, B.A. Chabner, The National Cancer Institute: cancer drug discovery and development program, *Semin. Oncol.*, 1992, pp. 622-638.
- [27] (a) V.N. Shinde, S. Dhiman, R. Krishnan, D. Kumar, A. Kumar, Synthesis of imidazopyridine-fused indoles via one-pot sequential Knoevenagel condensation and cross dehydrogenative coupling, *Org. Biomol. Chem.*, 16 (2018) 6123-6132; (b) J. John, J. Thomas, N. Parekh, W. Dehaen, Tandem Organocatalyzed Knoevenagel Condensation/1,3-Dipolar Cycloaddition towards Highly Functionalized Fused 1,2,3-Triazoles, *Eur. J. Org. Chem.*, 2015 (2015) 4922-4930; (c) Y. Liu, G. Nie, Z. Zhou, L. Jia, Y. Chen, Copper-catalyzed oxidative cross-dehydrogenative coupling/oxidative cycloaddition: Synthesis of 4-acyl-1,2,3-triazoles, *J. Org. Chem.*, 82 (2017) 9198-9203; (d) V.D. Bock, H. Hiemstra, J.H. Van Maarseveen, CuI-catalyzed alkyne-azide "click" cycloadditions from a mechanistic and synthetic perspective, *Eur. J. Org. Chem.*, 2006 (2006) 51-68.
- [28] (a) C. Temperini, L. Messori, P. Orioli, C.D. Bugno, F. Animati, G. Ughetto, The crystal structure of the complex between a disaccharide anthracycline and the DNA hexamer d (CGATCG) reveals two different binding sites involving two DNA duplexes, *Nucleic Acids Res.*, 31 (2003) 1464-1469; (b) Schrödinger suite **2017-1**; Schrödinger, LLC: New York, **2017**.
- [29] P. Vardevanyan, A.P. Antonyan, M. Parsadanyan, H. Davtyan, A. Karapetyan, The binding of ethidium bromide with DNA: interaction with single-and double-stranded structures, *Exp. Mol. Med.*, 35 (2003) 527.

**Tables, Schemes and Figures**

**Table 1:** Optimization of reaction condition

**Table 2.** Substrate scope for the synthesis of fused 1,2,3-triazole derivatives

**Table 3** Growth inhibition of the tested compounds against NCI human cancer cell line panel at 10  $\mu$ M

**Scheme 1.** Previous Work on Indole/Triazole/Diazepine fused Skeletons

**Scheme 2.** A plausible mechanism for the piperidine catalyzed tandem Knoevenagel condensation and azide–alkyne 1,3-dipolar cycloaddition reaction

**Figure 1.** Examples of bioactive *N*-heterocycles containing fused triazoles and diazepines

**Figure 2.** ORTEP diagram of compound **3k** (CCDC 1875794).

**Figure 3.** Colony forming assay

**Figure 4.** Effect of compound **3a** on cell cycle was determined by PI staining using flow cytometric analysis

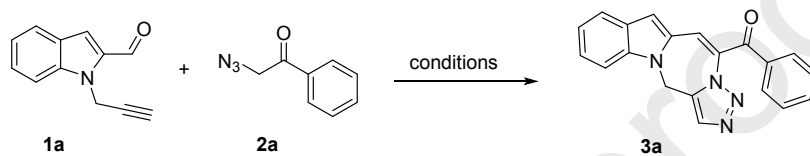
**Figure 5.** Dead cell apoptotic analysis was performed by Alexa flour 488-Annexin V and PI staining using flowcytometric analysis

**Figure 6.** Mitochondrial membrane potential was determined by JC-1 staining using flow cytometric analysis

**Figure 7.** DNA-intercalation studies

**Figure 7.** Docking poses for **3a** in DNA showing the intercalation-binding mode with PDB 1NAB

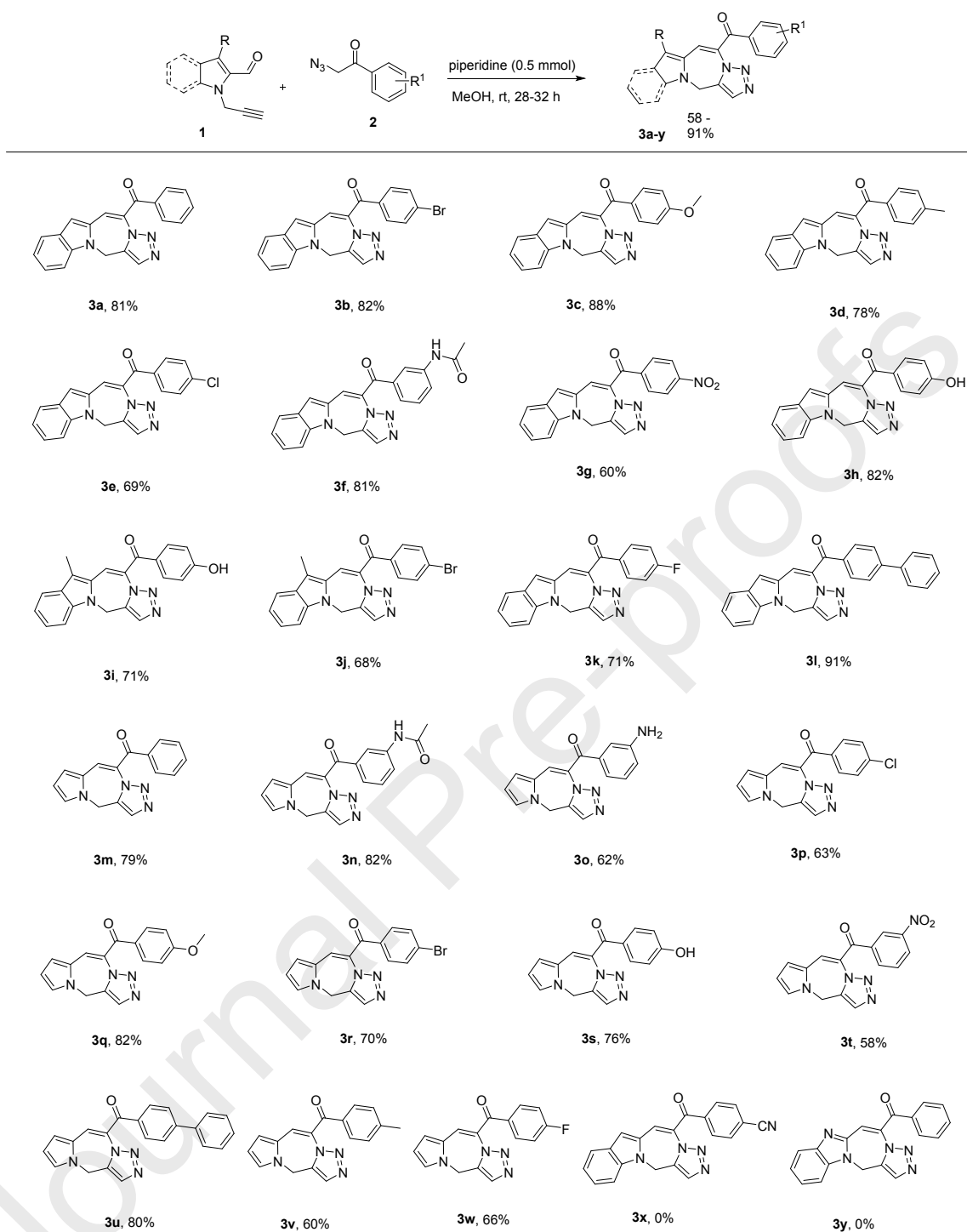
**Table 1:** Optimization of reaction condition<sup>a</sup>



Entry	Base(1.0 mmol)	Solvent	Time(h)	Yield <sup>b</sup> (%)
1	Cs <sub>2</sub> CO <sub>3</sub>	Ethanol	24	15
2	KOtBu	Ethanol	48	0
3	K <sub>2</sub> CO <sub>3</sub>	DMF	48	30
4	KOH	Methanol	48	32
5	NaOH	Methanol	48	28
6 <sup>c</sup>	K <sub>2</sub> CO <sub>3</sub>	Methanol	48	trace
7	TEA	Ethanol	30	62
8	TEA	Methanol	30	65
9	TEA	DMF	30	38
10	DBU	Methanol	30	56
11	Piperidine	Methanol	28	79
12	Piperidine	Methanol	32	78
<b>13</b>	<b>Piperidine (0.5)</b>	<b>Methanol</b>	<b>28</b>	<b>81</b>
14	Piperidine (0.4)	Methanol	30	72
15 <sup>c</sup>	Piperidine (0.5)	Methanol	28	42
16	Piperidine (0.5)	Water(PEG2000)	28	42

[a] Reaction conditions: **1a** (0.5 mmol) and **2b** (0.6 mmol), base (1.0 mmol), solvent (5 mL). [b] Yield of pure and isolated product. The reaction was performed at room temp. [c] The reaction was carried at reflux temperature (70 °C).

**Table 2.** Substrate scope for the synthesis of fused 1,2,3-triazole derivatives <sup>a,b</sup>



[a] Reaction conditions: **1** (0.5 mmol) and **2** (0.6 mmol), piperidine (0.5 mmol) in 5 mL of methanol. [b] An isolated yield was provided.

**Table 3** Growth inhibition of the tested compounds against NCI human cancer cell line panel at 10  $\mu\text{M}$

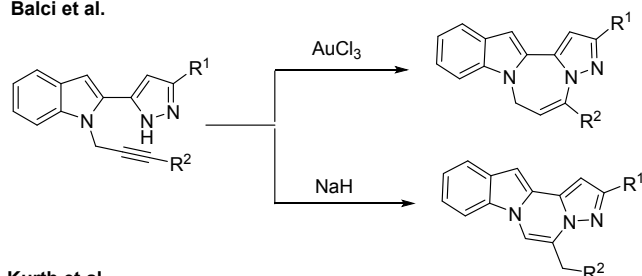
PANELNAME	CELLNAME	GIPRCNT				
		3a	3b	3f	3h	3u
<b>Leukemia</b>	CCRF-CEM	47.02	17.67	0.13	27.51	7.32
	HL-60(TB)	n. t.	24.11	n. t.	58.27	2.82
	K-562	78.57	17.69	17.25	89.00	51.06
	MOLT-4	57.87	21.77	11.11	55.43	6.18
	RPMI-8226	46.9	17.65	11.26	36.21	5.90
	SR	n. t.	5.91	n. t.	64.94	46.34
<b>Non-Small Cell Lung Cancer</b>						
<b>Cancer</b>	A549/ATCC	41.47	25.46	0.99	49.28	7.26
	EKVX	17.1	1.60	11.77	10.08	n. i.
	HOP-62	60.81	16.63	15.18	44.29	n. i.
	HOP-92	44.93	11.78	39.55	15.6	n. i.
	NCI-H226	21.87	17.3	14.55	14.86	16.71
	NCI-H23	26.37	0.52	1.46	24.43	0.87
	NCI-H322M	19.37	14.79	7.94	10.56	n. i.
	NCI-H460	69.14	5.47	n. i.	72.21	n. i.
	NCI-H522	90.32	48.77	17.14	63.34	29.4
<b>Colon Cancer</b>	COLO 205	41.18	n. i.	n. i.	24.49	n. i.
	HCC-2998	28.33	n. i.	n. i.	16.15	10.69
	HCT-116	73.33	13.71	9.21	53.63	3.24
	HCT-15	61.36	5.60	1.54	62.70	25.42
	HT29	92.20	10.16	n. i.	72.74	4.31
	KM12	66.19	2.96	21.14	70.5	31.55
	SW-620	71.46	n. i.	7.27	71.28	20.92
<b>CNS Cancer</b>	SF-268	41.22	12.47	0.24	28.05	4.39
	SF-295	43.70	n. i.	0.56	43.12	6.41
	SF-539	42.18	0.88	11.58	38.48	3.29
	SNB-19	67.77	7.5	15.74	36.80	9.03
	SNB-75	n. t.	23.15	n. t.	68.98	28.78
	U251	67.45	9.60	3.52	46.51	5.79
<b>Melanoma</b>						
	LOX IMVI	50.15	10.87	1.46	49.38	4.80
	MALME-3M	23.12	n. i.	n. i.	42.18	11.18
	M14	77.81	4.60	5.32	75.11	14.99
	MDA-MB-435	7.53 L*	3.41	22.05	7.67 L*	76.90
	SK-MEL-2	55.88	n. t.	n. i.	41.05	0.96

	SK-MEL-28	35.15	n. i.	8.38	33.23	9.45
	SK-MEL-5	54.24	9.56	10.16	45.77	4.03
	UACC-257	25.42	19.65	1.14	15.96	8.80
	UACC-62	55.55	23.57	33.75	67.12	28.90
<b>Ovarian Cancer</b>	IGROV1	55.37	8.63	21.42	58.93	7.25
	OVCAR-3	73.07	n. i.	2.13	79.45	1.70
	OVCAR-4	17.28	0.09	n. i.	18.74	10.12
	OVCAR-5	10.8	10.02	11.22	8.82	n. i.
	OVCAR-8	48.15	10.75	7.16	35.2	4.25
	NCI/ADR-RES	72.98	n. i.	n. i.	62.81	20.67
	SK-OV-3	32.21	11.86	n. i.	25.54	n. i.
<b>Renal Cancer</b>	786-0	30.93	n. i.	3.07	18.15	7.87
	A498	28.3	2.22	n. i.	n. i.	32.95
	ACHN	25.41	1.92	10.43	24.56	n. i.
	CAKI-1	42.05	7.66	17.67	62.46	15.32
	RXF 393	45.43	n. i.	10.46	41.04	3.64
	SN12C	49.72	n. i.	15.7	42.33	3.61
	TK-10	27.26	n. i.	n. i.	9.06	n. i.
	UO-31	35.16	35.01	43.10	36.91	15.41
<b>Prostate Cancer</b>	PC-3	52.29	28.99	22.93	37.6	16.18
	DU-145	14.42	n. i.	n. i.	10.07	n. i.
<b>Breast Cancer</b>	MCF7	64.84	7.72	15.86	65.73	25.43
	MDA-MB-231/ATCC	45.7	25.03	27.98	24.55	n. i.
	HS 578T	31.02	n. t.	16.73	50.62	17.2
	BT-549	62.55	n. i.	15.29	45.2	19.25
	T-47D	71.22	3.49	7.20	55.13	n. i.
	MDA-MB-468	94.02	1.98	26.22	37.75	3.50
<b>Human keratinocytes</b>	HaCaT	35.23	-	-	-	-

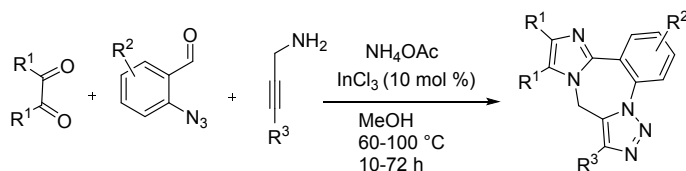
Highly potent, 90-100 % growth inhibition, 70-90% growth inhibition, 50-70% growth inhibition, 40-50 % growth inhibition, 30-40 % growth inhibition, L-lethality, \* Percentage of cells terminated/killed, n. t., not tested, n. i., no inhibition.

## Previous works

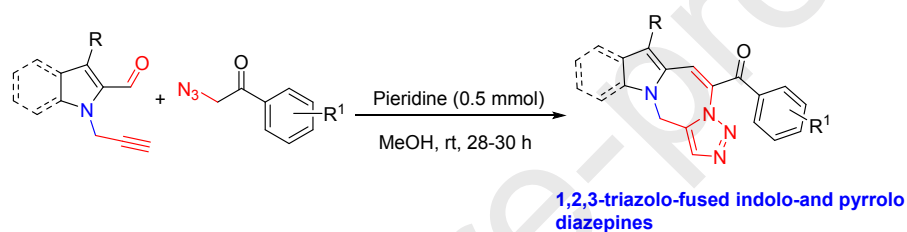
a) Balci et al.



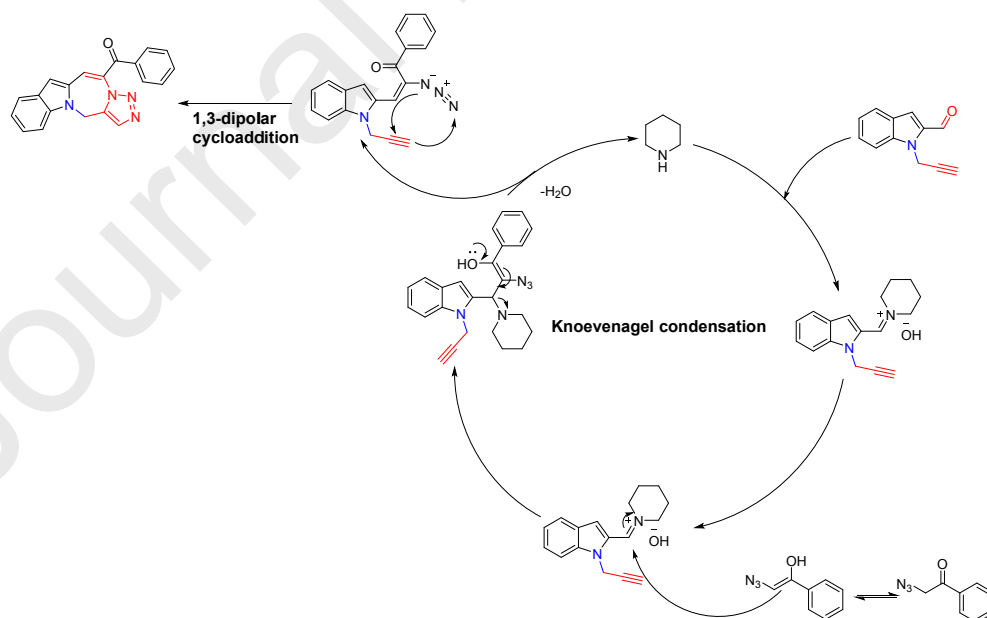
b) Kurth et al.



c) This work



Scheme 1. Previous Work on Indole/Triazole/Diazepine fused Skeletons.



Scheme 2. A plausible mechanism for the piperidine-catalyzed tandem Knoevenagel condensation and azide-alkyne 1,3-dipolar cycloaddition reaction [27].

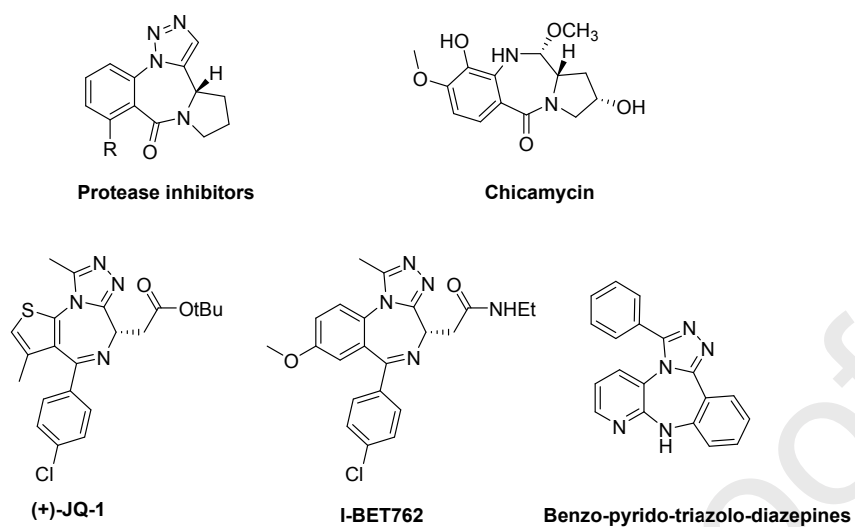


**Figure 1.** Examples of bioactive N-heterocycles containing fused triazoles and diazepines.

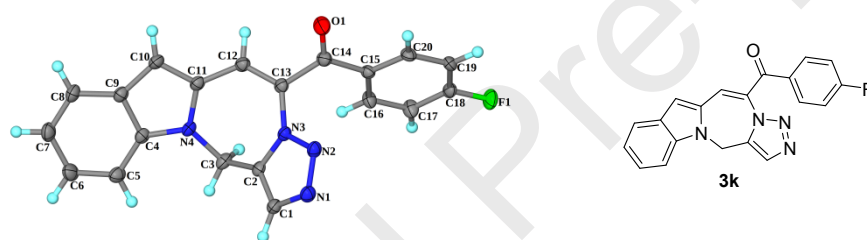


**Figure 2.** ORTEP diagram of compound **3k** (CCDC 1875794).

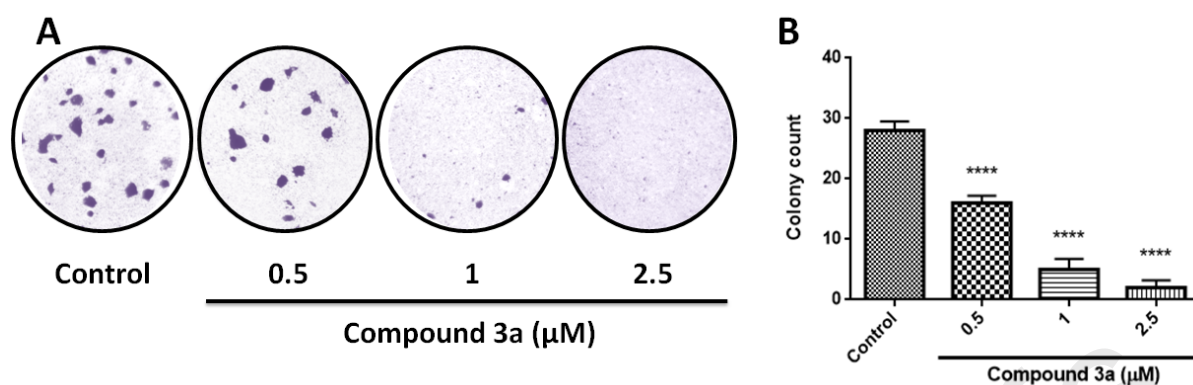


**Figure 3.** Colony forming assay. (A) Photographical images of colonies were taken after 12 days of compound **3a** treatment. (B) The number of colonies in unit area was calculated and represented as graph chart. Data represent as mean  $\pm$  SEM (n=3 independent experiments).

\*\*\*\* $P < 0.0001$  is significantly different from the control group.

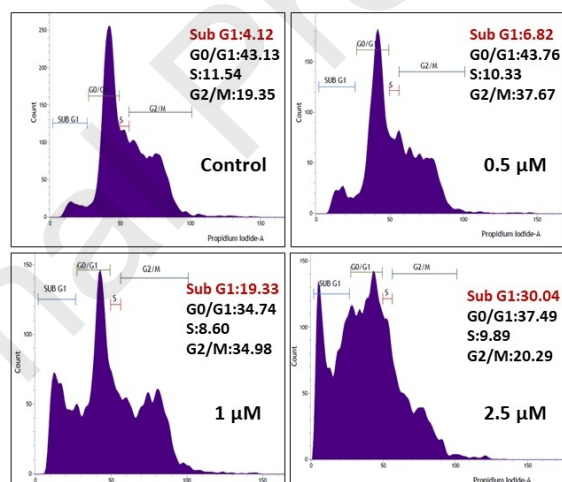


**Figure 4.** Effect of compound **3a** on cell cycle was determined by PI staining using flow cytometric analysis.

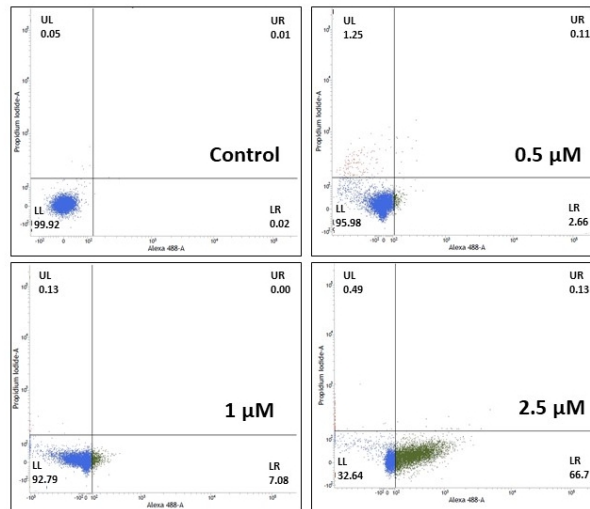


**Figure 5.** Dead cell apoptotic analysis was performed by Alexa flour 488-Annexin V and PI staining using flowcytometric analysis.

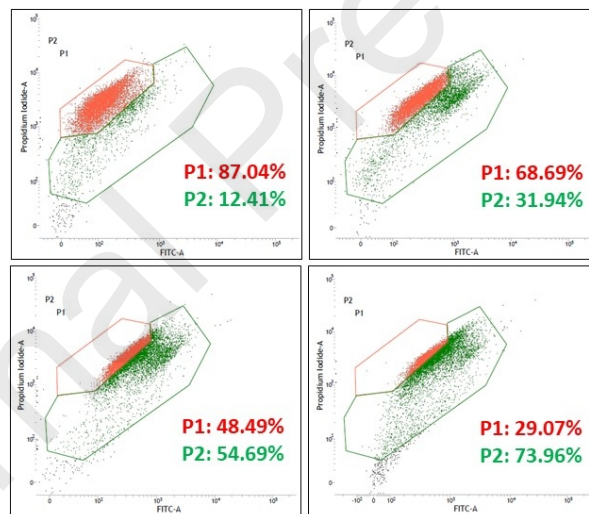


**Figure 6.** Mitochondrial membrane potential was determined by JC-1 staining using flow cytometric analysis.

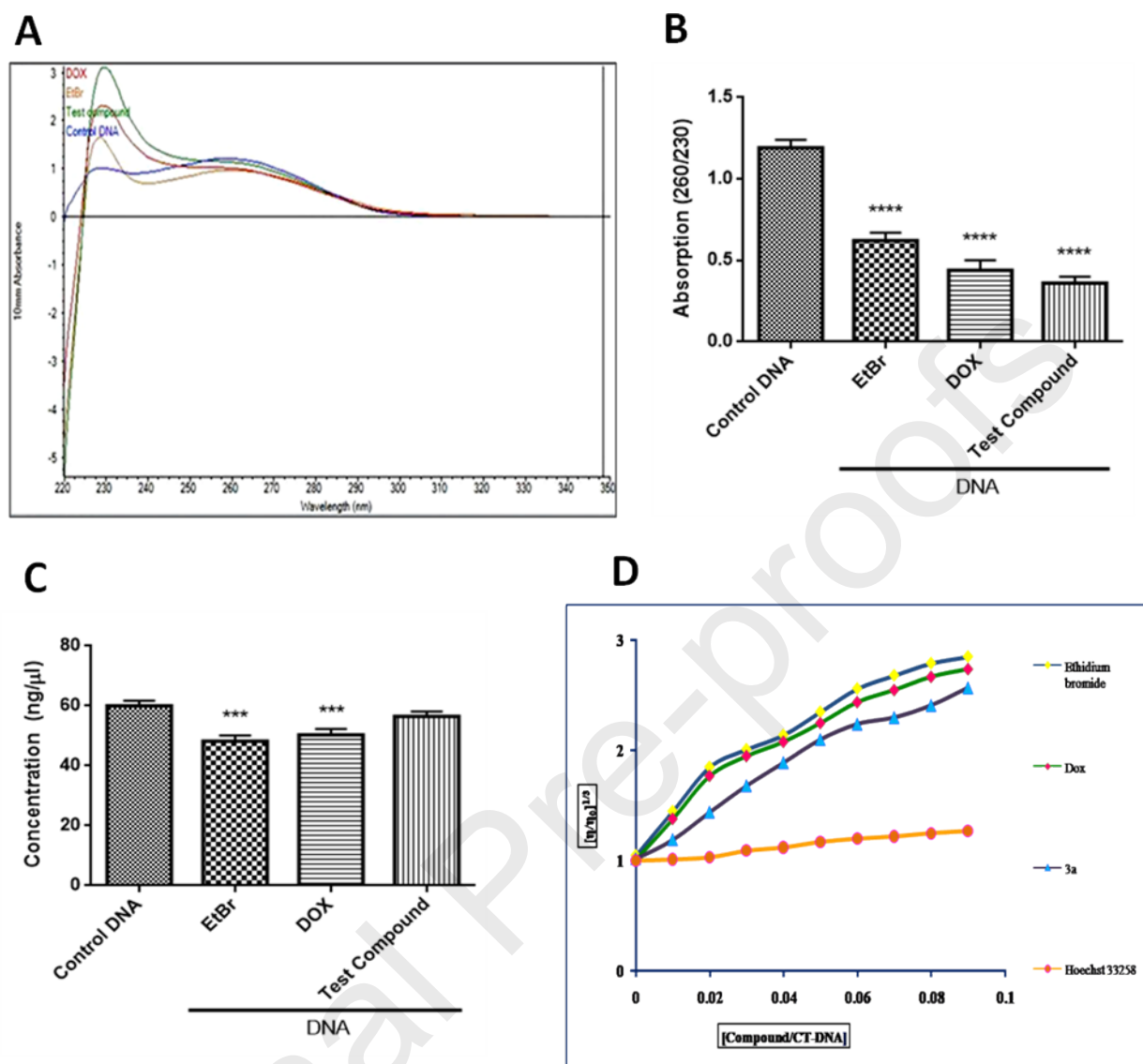


**Figure 7.** DNA-intercalation studies. (A) Spectrophotometric analysis was performed by nanodrop spectrophotometer. (B) The absorbance at 260/230 nm and (C) concentration and DNA was determined after the 10 min of incubation of DNA with test compound **3a** and EtBr and DOX (Doxorubicin). (D) Relative viscosity studies were performed to determine the DNA intercalation, where Hoechst-33258, DOX and EtBr used as reference standards. Here, Hoechst 33258 is employed as minor groove binder. Data represent as mean  $\pm$  SEM ( $n=3$  independent experiments). \*\*\* $P<0.001$  and \*\*\*\* $P<0.0001$  are significantly different from the control DNA group.

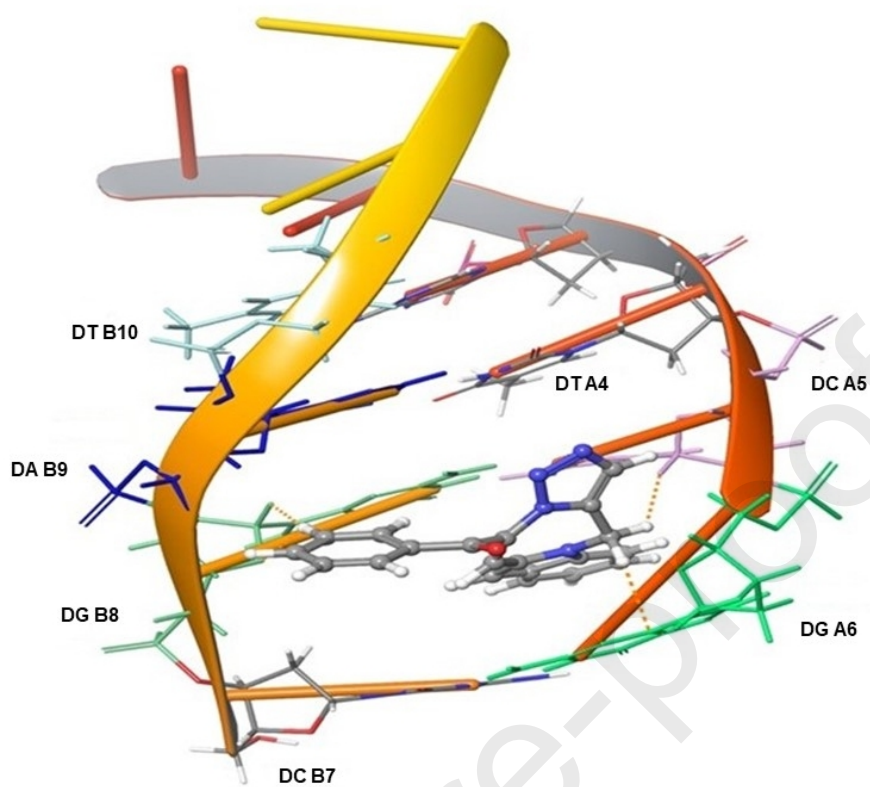


**Figure 8.** Docking poses for compound **3a** (element) in DNA showing the intercalation-binding mode with PDB 1NAB.

# **Facile synthesis of 1,2,3-triazole-fused Indolo- and Pyrrolo[1,4]diazepines, DNA-binding and evaluation of their anticancer activity**

Jitendra Gour,<sup>a</sup> Srikanth Gatadi,<sup>a</sup> Venkatesh Pooladanda,<sup>b</sup> Shaik Mahammad Ghouse,<sup>a</sup>

Satyaveni Malasala,<sup>a</sup> Y.V. Madhavi,<sup>a</sup> Chandraiah Godugu,<sup>b</sup> and Srinivas Nanduri\*<sup>a</sup>

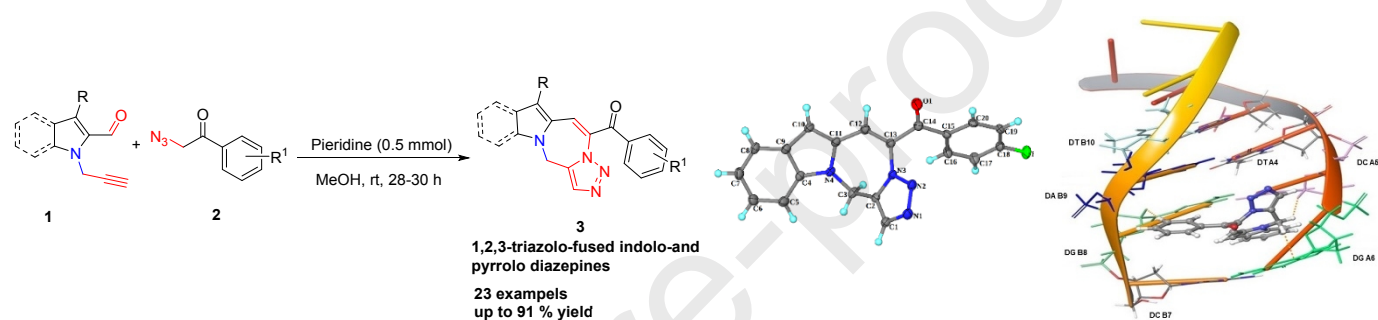
## **Conflicts of interest**

The authors declare no competing financial interest.

# Facile synthesis of 1,2,3-triazole-fused Indolo- and Pyrrolo[1,4]diazepines, DNA-binding and evaluation of their anticancer activity

Jitendra Gour,<sup>a</sup> Srikanth Gatadi,<sup>a</sup> Venkatesh Pooladanda,<sup>b</sup> Shaik Mahammad Ghouse,<sup>a</sup>

Satyaveni Malasala,<sup>a</sup> Y.V. Madhavi,<sup>a</sup> Chandraiah Godugu,<sup>b</sup> and Srinivas Nanduri\*<sup>a</sup>



- Metal free-synthesis
- Broad substrate scope
- New frameworks
- Anti-cancer activity
- DNA-intercalation ability

## Facile synthesis of 1,2,3-triazole-fused Indolo- and Pyrrolo[1,4]diazepines, DNA-binding and evaluation of their anticancer activity

Jitendra Gour,<sup>a</sup> Srikanth Gatadi,<sup>a</sup> Venkatesh Pooladanda,<sup>b</sup> Shaik Mahammad Ghouse,<sup>a</sup> Satyaveni Malasala,<sup>a</sup> Y.V. Madhavi,<sup>a</sup> Chandraiah Godugu,<sup>b</sup> and Srinivas Nanduri\*<sup>a</sup>

### Highlights:

- This work demonstrates a new approach for the synthesis of 1,2,3-triazole-fused indolo- and pyrrolo[1,4]diazepines.
- The reaction proceeds through an initial Knoevenagel condensation followed by intramolecular azide–alkyne cycloaddition reaction at room temperature without metal-catalyst in one-pot operation.
- The synthesized compounds were evaluated for their cytotoxic potential against a panel of 60 cancer cell lines at NCI.
- Compounds **3a** and **3h** exhibited broad spectrum potent inhibitory activity against all nine subpanels of cancer cell lines.
- Cell cycle analysis indicated that they inhibit the cell cycle at sub G1 phase.
- The DNA- nano drop method, viscosity experiment and docking studies suggested these compounds possess DNA binding affinity.